Parameter Estimation Bounds and Preamble Designs for SOQPSK Waveforms

Andre Tkacenko* **and Baris I. Erkmen***

In this paper, we derive joint parameter estimation bounds for the symbol timing offset, carrier phase, and carrier frequency offset for any shaped offset quadrature phase shift keying (SOQPSK) waveform. Specifically, we calculate the conditional Cramér-Rao bound (CCRB) for a known given data sequence and compare this to the modified Cramér-Rao bound (MCRB) for the case in which the data pattern is unknown and random. This allows us to assess the performance of candidate preamble waveforms for parameter acquisition. We show how to simplify the CCRB when the preamble waveform is periodic and compare the CCRB performance of several candidate preambles to the MCRB. For the Telemetry Group (TG) variant of SOQPSK (i.e., SOQPSK-TG), we specifically show that certain candidate preambles can offer substantial improvements over the MCRB in terms of symbol timing offset estimation with negligible adverse impact on the estimation of the carrier phase and carrier frequency offset.

I. Introduction

In an effort to meet the emerging needs of the telemetry based requirements for Department of Defense (DoD) test ranges, the Central Test and Evaluation Investment Program (CTEIP) of the DoD launched the integrated Network Enhanced Telemetry (iNET) program. To that end, the iNET Communication Link Standard Working Group (CLSWG) has made recommendations for the physical layer waveform to be used, including both single and multiple carrier signal formats [1]. For the single carrier physical layer modulation format [1], the iNET CLSWG has adopted a shaped offset quadrature phase shift keying (SOQPSK) constant envelope waveform [2]. Specifically, the iNET CLSWG has chosen the telemetry group (TG) variant of SOQPSK (i.e., SOQPSK-TG) [3, 4], on account of its spectral compactness. This property, coupled with the small

*Communication Architectures and Research Section

The research described in this publication was carried out by the Jet Propulsion Laboratory, California Institute of Technology, under a contract with the National Aeronautics and Space Administration.

amount of spectral regrowth due to nonlinear transmitter power amplification inherent of constant envelope waveforms, makes SOQPSK-TG a well suited modulation format to support a variety of test articles with a minimal amount of adjacent channel interference.

Furthermore, the iNET CLSWG has called for the use of a time division multiple access (TDMA) based asynchronous burst mode frame structure for the single carrier waveform [1]. At the beginning of each frame is a set of bits, called the preamble, allocated to aid in demodulator acquisition. This acquisition is to account for carrier phase/frequency offsets as well as symbol timing/clock offsets. Currently, the standard has proposed the use of a 128-bit preamble [1], but has not specified what this bit sequence should be.

In this paper, we focus on the joint estimation of the symbol timing offset, carrier phase, and carrier frequency offset for SOQPSK. The estimation model considered for these parameters is a discrete-time type obtained by sampling the underlying continuous-time waveform. For this parameter vector, we first derive the conditional *Fisher information matrix* (FIM) [5] used to calculate the conditional Cramér-Rao bound (CCRB) [5] for a known data sequence. We then compute the average FIM used to obtain the modified Cramér-Rao bound (MCRB) [6, 7] for the case of an unknown random data pattern.

Afterwards, we show how to simplify the conditional FIM for the case of a periodic preamble waveform. With these simplifications in effect, we compare the parameter estimation performances of several candidate periodic preambles (in terms of the CCRB) to those dictated by the MCRB for SOQPSK-TG. Specifically, certain preambles are shown to exhibit significant improvements over the MCRB in terms of symbol timing offset estimation with only minor deleterious effects on the estimation of the carrier phase and carrier frequency offset (less than 0.05 dB in bit signal-to-noise ratio (SNR)).

A. Outline

In Section II, we review the SOQPSK waveform signal model characteristics, including the frequency pulse function used for SOQPSK-TG. There, we introduce *dilated* pulses used to simplify subsequent mathematical analysis. In Section III, we review the parameter estimation model for the symbol timing offset, carrier phase, and carrier frequency offset. From the continuous-time waveform model stipulated in Section III.A, a discrete-time signal model is derived in Section III.B based on sampling. In Section IV, we review optimal lower bounds for estimating the parameters jointly. Specifically, in Section IV.A, we recall the conditional FIM and show its relation to the CCRB, in Section IV.B, we introduce the average FIM and the MCRB, and finally in Section IV.C, we review the unconditional FIM and the true underlying Cramér-Rao bound (CRB) [5]. In Section V, we derive the conditional FIM for a given data pattern. The average FIM, which is simply the conditional FIM averaged over all possible data sequences, is calculated in Section VI. In Section VII, we show how to simplify the conditional FIM for the case of a periodic preamble waveform. There, we use the results obtained for the average FIM in Section VI to aid in the choice of a suitable preamble sequence. In Section VIII, we show performance bounds for several candidate preambles and compare these bounds with those obtained

from the MCRB. There, we show that certain candidate preambles are able to achieve better estimation performance with respect to symbol timing with negligible adverse impact on carrier phase and carrier frequency offset estimation. Concluding remarks are made in Section IX. Finally, in the Appendix, we reveal the relationship between the true unconditional CRB and MCRB.

B. Notations

Standard signal processing notations as in [8] are used. In particular, parentheses and square brackets are used for continuous-time and discrete-time function arguments, respectively. As an example, $x(t)$ would denote a continuous-time function for $t \in \mathbb{R}$, whereas $y[n]$ would denote a discrete-time function for $n \in \mathbb{Z}$. For notational convenience, discrete-time function arguments will sometimes be written as a subscript, so that $y[n]$ may be alternately expressed as y_n.

Vector/matrix notations used are as in [9]. Specifically, boldface lowercase letters (such as $\mathbf{v}$) will be used to denote vectors, whereas boldface uppercase letters (such as $\mathbf{A}$) will be used to denote matrices. In addition, the (k,ℓ)-th element of a matrix $\mathbf{A}$ will be denoted as $[\mathbf{A}]_{k,\ell}$. The transpose and conjugate transpose operators will be represented by the superscripts ^{T} and †, respectively.

Statistical notations used are as in [5]. In particular, a hat will be used to denote an estimate of a parameter. For example, if θ is a parameter to be estimated, then $\widehat{\theta}$ would denote an estimate of θ. Furthermore, the expectation operator with respect to a random vector $\mathbf{x}$ will be denoted as $E_{\mathbf{x}}[\cdot]$. For example, if $p_{\mathbf{x}}(\boldsymbol{x})$ denotes the probability density function (pdf) of $\mathbf{x}$, then we have

$$E_{\mathbf{x}}[f(\mathbf{x})] = \int_{\mathcal{R}} p_{\mathbf{x}}(\boldsymbol{x}) f(\boldsymbol{x})\, d\boldsymbol{x}$$

for some function $f(\boldsymbol{x})$, where $\mathcal{R}$ denotes the support region of integration of the pdf $p_{\mathbf{x}}(\boldsymbol{x})$.

To make subsequent analysis less cumbersome, we will introduce *dilated* pulse shapes, which are simply traditional pulse functions that have been dilated by the symbol interval length and possibly scaled to remove any dependency on the symbol rate. All dilated pulse shapes will be denoted by an overline. For example, if $p(t)$ denotes the following unit-energy non-return to zero (NRZ) pulse shape [10] for a symbol interval length of T_{sym}

$$p(t) \triangleq \begin{cases} \frac{1}{\sqrt{T_{\text{sym}}}}, & -\frac{T_{\text{sym}}}{2} \le t < \frac{T_{\text{sym}}}{2} \\ 0, & \text{otherwise} \end{cases}$$

then a suitable dilated pulse shape would be $\overline{p}(x) \triangleq \sqrt{T_{\text{sym}}}\, p(xT_{\text{sym}})$. In this case, we have

$$\overline{p}(x) = \begin{cases} 1, & -\frac{1}{2} \le x < \frac{1}{2} \\ 0, & \text{otherwise} \end{cases}$$

which does not depend upon the symbol interval T_{sym}.

II. SOQPSK Waveform Characteristics

The transmitted continuous-time complex baseband analog signal corresponding to an SOQPSK waveform is of the following form [11]:

$$s(t) \triangleq \sqrt{\frac{E_b}{T_b}} \exp\left\{ j2\pi h \sum_{k\in\mathbb{Z}} \alpha_k q(t - kT_b) \right\} \tag{1}$$

Here, we have the following.

$$\begin{aligned} E_b &= \text{energy per bit} \\ T_b &= \text{bit duration} \\ h &= \text{modulation index } (h = 1/2 \text{ for SOQPSK-TG}) \\ \{\alpha_k\} &= \text{ternary symbol stream } (\alpha_k \in \{-1, 0, 1\}) \\ q(t) &= \text{phase pulse of SOQPSK} = \int_{-\infty}^{t} f(\tau)\, d\tau \\ f(t) &= \text{frequency pulse of SOQPSK} \end{aligned}$$

In order for the demodulated constellation corresponding to Equation (1) to conform to a conventional offset quadrature phase shift keying (OQPSK) constellation, as desired here, the mapping between the in-phase and quadrature bits to the ternary symbol stream $\{\alpha_k\}$ must be carried out properly. For SOQPSK, this is done as follows. Let $\{b_{I,k}\}$ and $\{b_{Q,k}\}$ denote, respectively, the in-phase and quadrature bit streams, where we have $b_{I,k}, b_{Q,k} \in \{0, 1\}$ for all k. These streams are then interleaved into a serial bit stream $\{b_k\}$ via the following mapping:

$$b_k = \begin{cases} b_{I,\frac{k}{2}}\,, & k \text{ even} \\ b_{Q,\frac{k-1}{2}}\,, & k \text{ odd} \end{cases} \tag{2}$$

Then, the serial bit stream $\{b_k\}$ is mapped to the ternary symbol stream $\{\alpha_k\}$ as follows [2, 3]:

$$\alpha_k = (-1)^{k+1} \left(2b_{k-1} - 1\right) \left(b_k - b_{k-2}\right) \tag{3}$$

The phase and frequency pulses $q(t)$ and $f(t)$ are implicitly parameterized by the bit interval T_b [2, 3]. In order to simplify further analysis here, we define the following dilated pulse shapes $\overline{q}(x)$ and $\overline{f}(x)$ as given below

$$\overline{q}(x) \triangleq q(xT_b)\ ,\ \overline{f}(x) \triangleq T_b f(xT_b) \tag{4}$$

It can be shown that the dilated pulses defined in Equation (4) do not depend upon the value of T_b chosen here. With the definitions given in Equation (4), the complex baseband signal $s(t)$ from Equation (1) becomes the following:

$$s(t) = \sqrt{\frac{E_b}{T_b}} \exp\left\{ j2\pi h \sum_{k\in\mathbb{Z}} \alpha_k \overline{q}\left(\frac{t}{T_b} - k\right) \right\} \tag{5}$$

where we have

$$\overline{q}(x) = \int_{-\infty}^{x} \overline{f}(\lambda)\, d\lambda \tag{6}$$

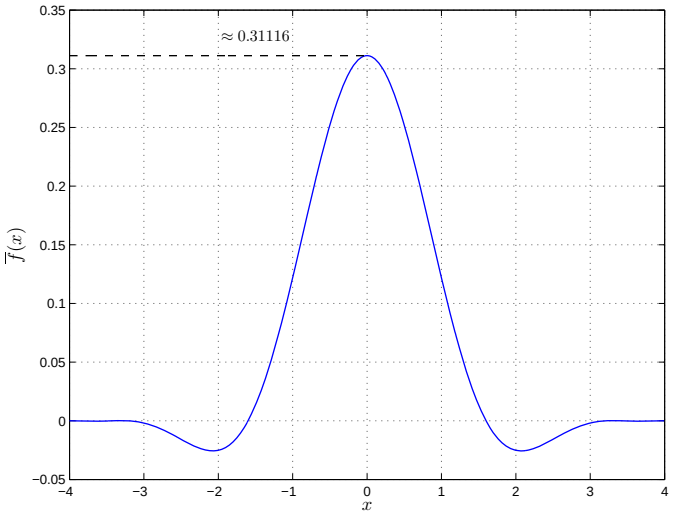

Figure 1. Plot of the dilated frequency pulse $\overline{f}(x)$ corresponding to SOQPSK-TG.

For SOQPSK-TG, the frequency pulse is a product of a raised cosine frequency-domain window and time-domain window [2] and is given by

$$\overline{f}(x) \triangleq A \frac{\cos\left(\frac{\pi\beta_1\beta_2 x}{2}\right)}{1 - 4\left(\frac{\beta_1\beta_2 x}{2}\right)^2} \operatorname{sinc}\left(\frac{\beta_2 x}{2}\right) \overline{w}(x) \tag{7}$$

where A is chosen to make $\int_{-\infty}^{\infty} \overline{f}(x)\, dx = 1/2$ and $\overline{w}(x)$ is given by the following expression:

$$\overline{w}(x) = \begin{cases} 1\,, & \left|\frac{x}{2}\right| < \gamma_1 \\ \frac{1}{2}\left[1 + \cos\left(\frac{\pi}{\gamma_2}\left(\frac{x}{2} - \gamma_1\right)\right)\right], & \gamma_1 \le \left|\frac{x}{2}\right| < \gamma_1 + \gamma_2 \\ 0\,, & \left|\frac{x}{2}\right| \ge \gamma_1 + \gamma_2 \end{cases}$$

Here, β_1, β_2 are parameters for the frequency-domain window which control the bandwidth and roll-off, whereas γ_1, γ_2 are parameters for the time-domain window which control the duration and roll-off. For SOQPSK-TG specifically, we have $\beta_1 = 7/10$, $\beta_2 = 5/4$, $\gamma_1 = 3/2$, and $\gamma_2 = 1/2$ [3, 4]. In this case, $\overline{f}(x)$ is only nonzero over the region $-4 < x < 4$. A plot of $\overline{f}(x)$ for SOQPSK-TG is shown in Figure 1.

For simplicity of subsequent mathematical analysis, we will define the *dilated normalized frequency trajectory function* $\overline{p}(x)$ as follows:

$$\overline{p}(x) \triangleq \sum_{k \in \mathbb{Z}} \alpha_k \overline{f}(x - k) \tag{8}$$

From Equations (6) and (8), it can be seen that we have

$$\overline{p}(x) = \sum_{k \in \mathbb{Z}} \alpha_k \frac{d}{dx}\left\{\overline{q}(x - k)\right\} = \frac{d}{dx}\left\{\sum_{k \in \mathbb{Z}} \alpha_k \overline{q}(x - k)\right\} \tag{9}$$

This property will prove useful when deriving optimal bounds for joint parameter estimation for SOQPSK.

III. Parameter Estimation Model

Here, we will consider the problem of jointly estimating three unknown deterministic parameters of an SOQPSK transmitted waveform corrupted by an additive noise: namely the symbol timing offset, carrier phase, and carrier frequency offset. Starting from a continuous-time complex baseband model, we will derive a corresponding discrete-time model based on sampling the underlying waveform. Then, with this discrete-time model, we will be able to statistically characterize the received set of samples and subsequently derive optimal lower bounds for the joint estimation of the three unknown parameters.

A. Continuous-Time Waveform Model

We will assume that the received complex baseband signal consists of the original transmitted signal from Equation (5) with an unknown deterministic symbol timing offset, carrier phase, and carrier frequency offset, corrupted by a circular complex additive white Gaussian noise (AWGN) process [10]. Prior to sampling the baseband signal at the analog-to-digital converter (ADC), it is filtered by an anti-aliasing filter to limit the bandwidth of the incoming signal to half the sampling rate. Here, we will assume that the anti-aliasing filter has no effect on the transmitted SOQPSK signal and only filters the AWGN process, which is approximately true assuming the sampling rate is sufficiently larger than the SOQPSK symbol rate [9]. With this assumption, the continuous-time complex baseband signal seen at the input to the ADC is given by the following expression:

$$y(t) = e^{j2\pi\left(\left(\frac{\nu}{T_b}\right)t+\phi\right)} s(t - \epsilon T_b) + \eta(t) \tag{10}$$

Here, we have the following.

$$\begin{aligned} y(t) &= \text{received baseband signal at the ADC input} \\ \eta(t) &= \text{bandlimited Gaussian noise process} \\ \epsilon &= \text{normalized symbol timing offset} \\ \phi &= \text{normalized carrier phase} \\ \nu &= \text{normalized carrier frequency offset} \end{aligned}$$

The noise process $\eta(t)$ is a continuous-time zero-mean circular complex bandlimited Gaussian process [10] with power spectral density (psd) [9] $S_{\eta\eta}(j2\pi F)$ given by

$$S_{\eta\eta}(j2\pi F) = \begin{cases} N_0\,, & -\frac{1}{2T_s} \leq F < \frac{1}{2T_s} \\ 0\,, & \text{otherwise} \end{cases} \tag{11}$$

where N_0 is the original AWGN spectral density and T_s is the ADC sampling interval.

Here, we are interested in the joint estimation of the three unknown deterministic parameters ϵ, ϕ, and ν. In other words, we are interested in estimating the 3×1 vector $\boldsymbol{\theta}$

defined below as follows:

$$\boldsymbol{\theta} \triangleq \begin{bmatrix} \epsilon \\ \phi \\ \nu \end{bmatrix} = \begin{bmatrix} \theta_0 \\ \theta_1 \\ \theta_2 \end{bmatrix} \tag{12}$$

We will consider estimating $\boldsymbol{\theta}$ from a sampled version of the continuous-time waveform $y(t)$ from Equation (10) described below.

B. Discrete-Time Signal Model

A discrete-time model is obtained by uniformly sampling the analog ADC input signal from Equation (10) at the sampling rate $1/T_s$ and collecting N observations. This leads to the model

$$y_m = s_m + w_m\,,\ m = 0, 1, \ldots, N-1 \tag{13}$$

where, we have $y_m \triangleq y(mT_s)$, $s_m \triangleq e^{j2\pi\left(\left(\frac{\nu}{T_b}\right)(mT_s)+\phi\right)} s(mT_s - \epsilon T_b)$, and $w_m \triangleq \eta(mT_s)$. Here, w_m is a discrete-time zero-mean circular complex AWGN process [10] with variance $\sigma^2 = \frac{N_0}{T_s}$.

Prior to proceeding with any subsequent developments, we will introduce three dimensionless quantities which will aid in the analysis. First, to help remove any explicit dependencies upon either the bit interval T_b or the sampling interval T_s, we will define the following quantity K:

$$K \triangleq \frac{T_b}{T_s} \tag{14}$$

Note that K as given in Equation (14) corresponds to the number of samples per bit. With K defined as in Equation (14), the signal sample s_m from above simplifies to the following expression:

$$s_m = e^{j2\pi\left(\left(\frac{\nu}{K}\right)m+\phi\right)} s\left(\left(\frac{m}{K} - \epsilon\right) T_b\right) \tag{15}$$

Second, we will define the number of bits observed to be L. In other words, we define L as follows:

$$L \triangleq \frac{N}{K} \tag{16}$$

Here, L as defined in Equation (16) is the total number of samples observed N divided by the number of samples per bit K and is thus the number of bits observed with the discrete-time model from Equation (13). We will assume here throughout that $L \in \mathbb{N}^+$ so that we always observe an integer number of bits.

Finally, let us consider the bit SNR [10], which we will denote here by ρ. Clearly, we have $\rho \triangleq \frac{E_b}{N_0}$, which can be simplified as shown below:

$$\rho = \frac{E_b}{N_0} = \frac{E_b}{\sigma^2 T_s} = \frac{E_b K}{\sigma^2 T_b} = \frac{\left(\frac{E_b}{T_b}\right) K}{\sigma^2} \tag{17}$$

In Equation (17), we used the definition of K given in Equation (14), along with the fact that the noise spectral density N_0 satisfies the relation $N_0 = \sigma^2 T_s$.

IV. Optimal Lower Bounds for Joint Parameter Estimation

To derive bounds for estimating the parameter vector $\boldsymbol{\theta}$ from the discrete-time signal model from Equation (13), we must first characterize the statistical properties of the model. Then, estimation performance can be delineated in terms of Cramér-Rao type bounds [5].

To that end, define the $N \times 1$ vectors $\mathbf{y} \triangleq \begin{bmatrix} y_0 & y_1 & \cdots & y_{N-1} \end{bmatrix}^T$ and $\mathbf{s}(\boldsymbol{\alpha};\boldsymbol{\theta}) \triangleq \begin{bmatrix} s_0 & s_1 & \cdots & s_{N-1} \end{bmatrix}^T$, where $\boldsymbol{\alpha}$ denotes the vector of ternary symbol stream values $\{\alpha_k\}$, which may be either random or known. Here, the notation $\mathbf{s}(\boldsymbol{\alpha};\boldsymbol{\theta})$ is used to emphasize the fact that the vector is a function of the ternary symbol stream $\boldsymbol{\alpha}$ and is parameterized by the unknown but deterministic vector $\boldsymbol{\theta}$ from Equation (12).

Let $p(\mathbf{y}|\boldsymbol{\alpha};\boldsymbol{\theta})$ denote the pdf of the random vector $\mathbf{y}$ given $\boldsymbol{\alpha}$ and parameterized by $\boldsymbol{\theta}$. As w_m from Equation (13) is a zero-mean circular complex AWGN process with variance σ^2, it follows that, given $\boldsymbol{\alpha}$, $\mathbf{y}$ is a circular complex Gaussian random vector [5] with mean $\mathbf{s}(\boldsymbol{\alpha};\boldsymbol{\theta})$ and covariance matrix $\sigma^2\mathbf{I}_N$. Hence, $p(\mathbf{y}|\boldsymbol{\alpha};\boldsymbol{\theta})$ is given by the following expression [5]:

$$p(\mathbf{y}|\boldsymbol{\alpha};\boldsymbol{\theta}) = \frac{1}{\pi^N \sigma^{2N}} \exp\left\{ -\frac{||\mathbf{y} - \mathbf{s}(\boldsymbol{\alpha};\boldsymbol{\theta})||^2}{\sigma^2} \right\} \tag{18}$$

A. Conditional FIM and the Conditional CRB

Given the ternary symbol stream $\boldsymbol{\alpha}$, the mean squared error performance of any unbiased estimator of $\boldsymbol{\theta}$ can be lower bounded by the *conditional CRB*, which is solely a function of the pdf $p(\mathbf{y}|\boldsymbol{\alpha};\boldsymbol{\theta})$ [5]. Specifically, let $\widehat{\boldsymbol{\theta}}(\mathbf{y}|\boldsymbol{\alpha})$ denote any unbiased estimator [5] of $\boldsymbol{\theta}$ for a given $\boldsymbol{\alpha}$, meaning that $E_{\mathbf{y}|\boldsymbol{\alpha}}\left[\widehat{\boldsymbol{\theta}}(\mathbf{y}|\boldsymbol{\alpha})\right] = \boldsymbol{\theta}$. Also, let $\mathbf{e}(\mathbf{y}|\boldsymbol{\alpha};\boldsymbol{\theta})$ denote the error between the true parameter and its estimate defined to be

$$\mathbf{e}(\mathbf{y}|\boldsymbol{\alpha};\boldsymbol{\theta}) \triangleq \boldsymbol{\theta} - \widehat{\boldsymbol{\theta}}(\mathbf{y}|\boldsymbol{\alpha})$$

Note that we have $E_{\mathbf{y}|\boldsymbol{\alpha}}\left[\mathbf{e}(\mathbf{y}|\boldsymbol{\alpha};\boldsymbol{\theta})\right] = \mathbf{0}$ as $\widehat{\boldsymbol{\theta}}(\mathbf{y}|\boldsymbol{\alpha})$ is an *unbiased* estimate of $\boldsymbol{\theta}$ here. Finally, let $\mathbf{C}_{\mathbf{ee}}(\boldsymbol{\theta}|\boldsymbol{\alpha})$ denote the covariance matrix of the error $\mathbf{e}(\mathbf{y}|\boldsymbol{\alpha};\boldsymbol{\theta})$, defined as follows:

$$\mathbf{C}_{\mathbf{ee}}(\boldsymbol{\theta}|\boldsymbol{\alpha}) \triangleq E_{\mathbf{y}|\boldsymbol{\alpha}}\left[\mathbf{e}(\mathbf{y}|\boldsymbol{\alpha};\boldsymbol{\theta})\mathbf{e}^{\dagger}(\mathbf{y}|\boldsymbol{\alpha};\boldsymbol{\theta})\right]$$

Then, for any unbiased estimator $\widehat{\boldsymbol{\theta}}(\mathbf{y}|\boldsymbol{\alpha})$ of $\boldsymbol{\theta}$, we have [5]

$$\mathbf{C}_{\mathbf{ee}}(\boldsymbol{\theta}|\boldsymbol{\alpha}) \geq \mathrm{CCRB}\left(\boldsymbol{\theta}|\boldsymbol{\alpha}\right) = \mathbf{F}^{-1}(\boldsymbol{\theta}|\boldsymbol{\alpha}) \tag{19}$$

where $\mathrm{CCRB}\left(\boldsymbol{\theta}|\boldsymbol{\alpha}\right)$ and $\mathbf{F}(\boldsymbol{\theta}|\boldsymbol{\alpha})$ denote, respectively, the *conditional Cramér-Rao bound* (CCRB) and *conditional Fisher information matrix* (FIM) of $\boldsymbol{\theta}$ given $\boldsymbol{\alpha}$ [5]. It should be noted and emphasized that the inequality in Equation (19) is a *matrix inequality* [12] which implicitly takes into account the effect that the parameters have on each other in terms of estimation performance. Here, the matrix inequality notation $\mathbf{A} \geq \mathbf{B}$ is

equivalent to saying that $(\mathbf{A}-\mathbf{B})$ is positive semidefinite [12]. The (k,ℓ)-th element of the conditional FIM $\mathbf{F}(\boldsymbol{\theta}|\boldsymbol{\alpha})$ is given by [5]

$$[\mathbf{F}(\boldsymbol{\theta}|\boldsymbol{\alpha})]_{k,\ell} = -E_{\mathbf{y}|\boldsymbol{\alpha}}\left[\frac{\partial^2}{\partial\theta_k\partial\theta_\ell}\ln p(\mathbf{y}|\boldsymbol{\alpha};\boldsymbol{\theta})\right],\ 0\le k,\ell\le 2 \tag{20}$$

From Equations (20) and (19), it can be seen that the conditional FIM $\mathbf{F}(\boldsymbol{\theta}|\boldsymbol{\alpha})$ and CCRB matrix $\text{CCRB}\,(\boldsymbol{\theta}|\boldsymbol{\alpha})$ are solely functions of the pdf $p(\mathbf{y}|\boldsymbol{\alpha};\boldsymbol{\theta})$. This establishes a lower bound on the mean squared error for parameter estimation based solely on the statistical properties of the received signal observation vector $\mathbf{y}$, given a ternary symbol stream $\boldsymbol{\alpha}$.

B. Average FIM and the Modified CRB

For cases in which the ternary symbol stream $\boldsymbol{\alpha}$ is not known and random, a figure of merit that is often used to assess the performance of an estimator for $\boldsymbol{\theta}$ is to average the FIM values from Equation (20) over each and every possible random realization of $\boldsymbol{\alpha}$. The inverse of this averaged FIM then yields what is known as the *modified Cramér-Rao bound* (MCRB) matrix [6, 7]. Specifically, the MCRB matrix is defined as

$$\text{MCRB}\,(\boldsymbol{\theta}) \triangleq \mathbf{G}^{-1}(\boldsymbol{\theta}) \tag{21}$$

where $\mathbf{G}(\boldsymbol{\theta})$ is the *average Fisher information matrix* whose (k,ℓ)-th element is given by the following expression:

$$[\mathbf{G}(\boldsymbol{\theta})]_{k,\ell} = -E_{\mathbf{y},\boldsymbol{\alpha}}\left[\frac{\partial^2}{\partial\theta_k\partial\theta_\ell}\ln p(\mathbf{y}|\boldsymbol{\alpha};\boldsymbol{\theta})\right],\ 0\le k,\ell\le 2 \tag{22}$$

Comparing Equations (22) and (20), it can be easily seen that we have

$$\mathbf{G}(\boldsymbol{\theta}) = E_{\boldsymbol{\alpha}}\left[\mathbf{F}(\boldsymbol{\theta}|\boldsymbol{\alpha})\right] \tag{23}$$

and so the average FIM $\mathbf{G}(\boldsymbol{\theta})$ is simply the conditional FIM $\mathbf{F}(\boldsymbol{\theta}|\boldsymbol{\alpha})$ averaged over the set of all possible random ternary symbol streams $\{\boldsymbol{\alpha}\}$.

Though the MCRB is not *per se* a bound on the performance of an estimator for $\boldsymbol{\theta}$, it is a useful figure of merit by which to assess the performance of a specific symbol stream $\boldsymbol{\alpha}$. In the case in which the parameter vector $\boldsymbol{\theta}$ is a scalar, the MCRB can be a beneficial tool to evaluate the effect of a specific value of $\boldsymbol{\alpha}$ on estimation performance. On account of the averaging used to calculate the MCRB, in this scalar case, some choices of $\boldsymbol{\alpha}$ must yield better performance than the MCRB, whereas others must yield inferior performance. While this intuition does not hold as such for the general vector case, the MCRB can nonetheless be used as a metric by which to compare the performance of CCRBs for various values of $\boldsymbol{\alpha}$.

C. Unconditional FIM and the CRB

When the ternary symbol stream $\boldsymbol{\alpha}$ is not known and random, the mean squared error performance of any unbiased estimator of $\boldsymbol{\theta}$ is lower bounded by the *unconditional CRB*,

which is only a function of the pdf of the received observation vector $\mathbf{y}$ parameterized by $\boldsymbol{\theta}$, which we denote here by $p(\mathbf{y};\boldsymbol{\theta})$ [5]. Analogous to the results from Section IV.A, let $\widehat{\boldsymbol{\theta}}(\mathbf{y})$ denote any unbiased estimator of $\boldsymbol{\theta}$ and define the error between the true parameter and its estimate to be $\mathbf{e}(\mathbf{y};\boldsymbol{\theta}) \triangleq \boldsymbol{\theta} - \widehat{\boldsymbol{\theta}}(\mathbf{y})$. If $\mathbf{C}_{\mathbf{ee}}(\boldsymbol{\theta})$ denotes the covariance matrix of the error given by

$$\mathbf{C}_{\mathbf{ee}}(\boldsymbol{\theta}) \triangleq E_{\mathbf{y}}\left[\mathbf{e}(\mathbf{y};\boldsymbol{\theta})\mathbf{e}^{\dagger}(\mathbf{y};\boldsymbol{\theta})\right]$$

then we have

$$\mathbf{C}_{\mathbf{ee}}(\boldsymbol{\theta}) \geq \mathrm{CRB}\left(\boldsymbol{\theta}\right) = \mathbf{H}^{-1}(\boldsymbol{\theta}) \tag{24}$$

where $\mathrm{CRB}\left(\boldsymbol{\theta}\right)$ and $\mathbf{H}(\boldsymbol{\theta})$ denote, respectively, the true unconditional CRB and unconditional FIM of $\boldsymbol{\theta}$ [5]. As with Equation (19), the inequality in Equation (24) is a matrix inequality [12]. The (k,ℓ)-th element of the unconditional FIM $\mathbf{H}(\boldsymbol{\theta})$ is given by [5]

$$[\mathbf{H}(\boldsymbol{\theta})]_{k,\ell} = -E_{\mathbf{y}}\left[\frac{\partial^2}{\partial\theta_k \partial\theta_\ell} \ln p(\mathbf{y};\boldsymbol{\theta})\right], \; 0 \leq k,\ell \leq 2 \tag{25}$$

From Equations (25) and (24), it can be seen that the unconditional FIM $\mathbf{H}(\boldsymbol{\theta})$ and CRB matrix $\mathrm{CRB}\left(\boldsymbol{\theta}\right)$ are solely functions of the pdf $p(\mathbf{y};\boldsymbol{\theta})$. This establishes a lower bound on the mean squared error for parameter estimation based solely on the statistical properties of the received signal observation vector $\mathbf{y}$.

In practice, it is often difficult or intractable to calculate the unconditional CRB. The reason for this is that it involves the unconditional pdf $p(\mathbf{y};\boldsymbol{\theta})$, which is often more cumbersome to work with than the conditional pdf $p(\mathbf{y}|\boldsymbol{\alpha};\boldsymbol{\theta})$. To see why this is the case, note that the unconditional pdf is given in terms of the conditional one via the following relationship [5]:

$$p(\mathbf{y};\boldsymbol{\theta}) = \int_{\mathcal{R}_{\boldsymbol{\alpha}}} p(\mathbf{y}|\boldsymbol{\alpha};\boldsymbol{\theta})\, p(\boldsymbol{\alpha})\, d\boldsymbol{\alpha} = E_{\boldsymbol{\alpha}}\left[\, p(\mathbf{y}|\boldsymbol{\alpha};\boldsymbol{\theta})\right] \tag{26}$$

Here, $p(\boldsymbol{\alpha})$ denotes the pdf of the ternary symbol stream $\boldsymbol{\alpha}$ and $\mathcal{R}_{\boldsymbol{\alpha}}$ denotes the region of support of this pdf [5]. Specifically for the SOQPSK signal model of Equation (13) considered here, calculating $p(\mathbf{y};\boldsymbol{\theta})$ from Equation (26) is intractable since the integration will degenerate into a sum of numerous terms over all possible ternary symbol stream values $\boldsymbol{\alpha}$ over the observation time set $\{t : t = mT_s - \epsilon T_b, 0 \leq m \leq N-1\}$.

One interesting property relating the unconditional CRB and the MCRB is that we have [6, 7]

$$\mathrm{MCRB}\left(\boldsymbol{\theta}\right) \leq \mathrm{CRB}\left(\boldsymbol{\theta}\right) \tag{27}$$

where the inequality in Equation (27) is a matrix inequality [12]. This property is proven in the Appendix.

V. Derivation of the Conditional FIM

From Equation (20), it can be seen that the conditional FIM is *Hermitian* [12], and so the only terms that must be calculated here are the six terms $[\mathbf{F}(\boldsymbol{\theta}|\boldsymbol{\alpha})]_{0,0}$, $[\mathbf{F}(\boldsymbol{\theta}|\boldsymbol{\alpha})]_{0,1}$, $[\mathbf{F}(\boldsymbol{\theta}|\boldsymbol{\alpha})]_{0,2}$, $[\mathbf{F}(\boldsymbol{\theta}|\boldsymbol{\alpha})]_{1,1}$, $[\mathbf{F}(\boldsymbol{\theta}|\boldsymbol{\alpha})]_{1,2}$, and $[\mathbf{F}(\boldsymbol{\theta}|\boldsymbol{\alpha})]_{2,2}$. Prior to focusing on simplifying each

of these terms individually, it is insightful to simplify the general expression of $[\mathbf{F}(\boldsymbol{\theta}|\boldsymbol{\alpha})]_{k,\ell}$ for the specific pdf $p(\mathbf{y}|\boldsymbol{\alpha};\boldsymbol{\theta})$ given in Equation (18). Starting with Equation (18), note that we have the following:

$$\begin{aligned}
\ln p(\mathbf{y}|\boldsymbol{\alpha};\boldsymbol{\theta}) &= -N\ln\left(\pi\sigma^2\right) - \frac{||\mathbf{y}-\mathbf{s}(\boldsymbol{\alpha};\boldsymbol{\theta})||^2}{\sigma^2} \\
&= -N\ln\left(\pi\sigma^2\right) - \frac{||\mathbf{y}||^2}{\sigma^2} - \frac{||\mathbf{s}(\boldsymbol{\alpha};\boldsymbol{\theta})||^2}{\sigma^2} + \frac{\mathbf{y}^\dagger\mathbf{s}(\boldsymbol{\alpha};\boldsymbol{\theta})}{\sigma^2} + \frac{\mathbf{s}^\dagger(\boldsymbol{\alpha};\boldsymbol{\theta})\mathbf{y}}{\sigma^2} \\
&= -N\ln\left(\pi\sigma^2\right) - \frac{||\mathbf{y}||^2}{\sigma^2} - \frac{N\left(\frac{E_b}{T_b}\right)}{\sigma^2} + \frac{\mathbf{y}^\dagger\mathbf{s}(\boldsymbol{\alpha};\boldsymbol{\theta})}{\sigma^2} + \frac{\mathbf{s}^\dagger(\boldsymbol{\alpha};\boldsymbol{\theta})\mathbf{y}}{\sigma^2} \qquad (28)
\end{aligned}$$

Here, Equation (28) follows from exploiting the constant envelope property of $s(t)$ from Equation (5) in Equation (15). Partially differentiating both sides of Equation (28) with respect to θ_ℓ followed by θ_k yields the following:

$$\frac{\partial^2}{\partial\theta_k\partial\theta_\ell}\ln p(\mathbf{y}|\boldsymbol{\alpha};\boldsymbol{\theta}) = \frac{1}{\sigma^2}\left[\mathbf{y}^\dagger\left(\frac{\partial^2}{\partial\theta_k\partial\theta_\ell}\mathbf{s}(\boldsymbol{\alpha};\boldsymbol{\theta})\right) + \left(\frac{\partial^2}{\partial\theta_k\partial\theta_\ell}\mathbf{s}(\boldsymbol{\alpha};\boldsymbol{\theta})\right)^\dagger\mathbf{y}\right] \qquad (29)$$

Now, as the expected value of the vector $\mathbf{y}$ is the signal component $\mathbf{s}(\boldsymbol{\alpha};\boldsymbol{\theta})$ (i.e., we have $E_{\mathbf{y}|\boldsymbol{\alpha}}[\mathbf{y}] = \mathbf{s}(\boldsymbol{\alpha};\boldsymbol{\theta})$), it follows that the (k,ℓ)-th element of the conditional FIM $\mathbf{F}(\boldsymbol{\theta}|\boldsymbol{\alpha})$ from Equation (20) simplifies to the following:

$$\begin{aligned}
[\mathbf{F}(\boldsymbol{\theta}|\boldsymbol{\alpha})]_{k,\ell} &= -\frac{1}{\sigma^2}\left[\mathbf{s}^\dagger(\boldsymbol{\alpha};\boldsymbol{\theta})\left(\frac{\partial^2}{\partial\theta_k\partial\theta_\ell}\mathbf{s}(\boldsymbol{\alpha};\boldsymbol{\theta})\right) + \left(\frac{\partial^2}{\partial\theta_k\partial\theta_\ell}\mathbf{s}(\boldsymbol{\alpha};\boldsymbol{\theta})\right)^\dagger\mathbf{s}(\boldsymbol{\alpha};\boldsymbol{\theta})\right] \\
&= -\frac{2}{\sigma^2}\mathrm{Re}\left\{\mathbf{s}^\dagger(\boldsymbol{\alpha};\boldsymbol{\theta})\left(\frac{\partial^2}{\partial\theta_k\partial\theta_\ell}\mathbf{s}(\boldsymbol{\alpha};\boldsymbol{\theta})\right)\right\} \\
&= -\frac{2}{\sigma^2}\sum_{m=0}^{N-1}\mathrm{Re}\left\{[\mathbf{s}(\boldsymbol{\alpha};\boldsymbol{\theta})]_m^* \cdot \frac{\partial^2}{\partial\theta_k\partial\theta_\ell}[\mathbf{s}(\boldsymbol{\alpha};\boldsymbol{\theta})]_m\right\} \\
&= -\frac{2}{\sigma^2}\sum_{m=0}^{N-1}\mathrm{Re}\left\{s_m^* \cdot \frac{\partial^2 s_m}{\partial\theta_k\partial\theta_\ell}\right\} = -\frac{2}{\sigma^2}\sum_{m=0}^{KL-1}\mathrm{Re}\left\{s_m^* \cdot \frac{\partial^2 s_m}{\partial\theta_k\partial\theta_\ell}\right\} \qquad (30)
\end{aligned}$$

Here, the last equality in Equation (30) follows from Equation (16). Finally, prior to simplifying specific terms of the conditional FIM, it is useful to compute the first order partial derivatives of s_m from Equation (15). Using Equation (12), we have the following after some algebraic manipulation:

$$\frac{\partial s_m}{\partial\theta_0} = \frac{\partial s_m}{\partial\epsilon} = -j2\pi h\,\overline{p}\left(\frac{m}{K}-\epsilon\right)s_m \qquad (31)$$

$$\frac{\partial s_m}{\partial\theta_1} = \frac{\partial s_m}{\partial\phi} = j2\pi s_m \qquad (32)$$

$$\frac{\partial s_m}{\partial\theta_2} = \frac{\partial s_m}{\partial\nu} = j2\pi\left(\frac{m}{K}\right)s_m \qquad (33)$$

A. Symbol Timing Offset/Symbol Timing Offset Cross Term

From Equation (30), the symbol timing offset/symbol timing offset cross term $[\mathbf{F}(\boldsymbol{\theta}|\boldsymbol{\alpha})]_{0,0}$ is given by the following:

$$[\mathbf{F}(\boldsymbol{\theta}|\boldsymbol{\alpha})]_{0,0} = -\frac{2}{\sigma^2}\sum_{m=0}^{KL-1}\mathrm{Re}\left\{s_m^* \cdot \frac{\partial^2 s_m}{\partial\theta_0^2}\right\} \qquad (34)$$

Now, using Equation (31), we have the following set of expressions:

$$\begin{aligned}
\frac{\partial^2 s_m}{\partial \theta_0^2} &= -(2\pi h)^2 \, \overline{p}^2\Big(\frac{m}{K} - \epsilon\Big) \, s_m + j2\pi h \, \overline{p}'\Big(\frac{m}{K} - \epsilon\Big) \, s_m \\
s_m^* \cdot \frac{\partial^2 s_m}{\partial \theta_0^2} &= -(2\pi h)^2 \left(\frac{E_b}{T_b}\right) \overline{p}^2\Big(\frac{m}{K} - \epsilon\Big) + j2\pi h \left(\frac{E_b}{T_b}\right) \overline{p}'\Big(\frac{m}{K} - \epsilon\Big) \qquad (35) \\
\mathrm{Re}\left\{ s_m^* \cdot \frac{\partial^2 s_m}{\partial \theta_0^2} \right\} &= -(2\pi h)^2 \left(\frac{E_b}{T_b}\right) \overline{p}^2\Big(\frac{m}{K} - \epsilon\Big) \qquad (36)
\end{aligned}$$

Here, Equation (35) follows from the constant envelope property $|s_m|^2 = \frac{E_b}{T_b}$, which in turn follows from Equations (15) and (5). Substituting Equation (36) into Equation (34) yields

$$[\mathbf{F}(\boldsymbol{\theta}|\boldsymbol{\alpha})]_{0,0} = \frac{2(2\pi h)^2 \left(\frac{E_b}{T_b}\right)}{\sigma^2} \sum_{m=0}^{KL-1} \overline{p}^2\Big(\frac{m}{K} - \epsilon\Big) \qquad (37)$$

Using Equation (17) in Equation (37) leads to the following simplified expression for the symbol timing offset/symbol timing offset cross term:

$$[\mathbf{F}(\boldsymbol{\theta}|\boldsymbol{\alpha})]_{0,0} = \frac{2(2\pi h)^2 \rho}{K} \sum_{m=0}^{KL-1} \overline{p}^2\Big(\frac{m}{K} - \epsilon\Big) \qquad (38)$$

As will be shown in Section VII, the dependency of $[\mathbf{F}(\boldsymbol{\theta}|\boldsymbol{\alpha})]_{0,0}$ in Equation (38) upon ϵ approximately goes away for a periodic waveform $\overline{p}(x)$.

B. Symbol Timing Offset/Carrier Phase Cross Term

From Equation (30), the symbol timing offset/carrier phase cross term $[\mathbf{F}(\boldsymbol{\theta}|\boldsymbol{\alpha})]_{0,1}$ is given by the following:

$$[\mathbf{F}(\boldsymbol{\theta}|\boldsymbol{\alpha})]_{0,1} = -\frac{2}{\sigma^2} \sum_{m=0}^{KL-1} \mathrm{Re}\left\{ s_m^* \cdot \frac{\partial^2 s_m}{\partial \theta_0 \partial \theta_1} \right\} \qquad (39)$$

Now, using Equations (32) and (31), we have the following set of expressions:

$$\begin{aligned}
\frac{\partial^2 s_m}{\partial \theta_0 \partial \theta_1} &= (2\pi)^2 h \, \overline{p}\left(\frac{m}{K} - \epsilon\right) s_m \\
s_m^* \cdot \frac{\partial^2 s_m}{\partial \theta_0 \partial \theta_1} &= (2\pi)^2 h \left(\frac{E_b}{T_b}\right) \overline{p}\left(\frac{m}{K} - \epsilon\right) \\
\mathrm{Re}\left\{ s_m^* \cdot \frac{\partial^2 s_m}{\partial \theta_0 \partial \theta_1} \right\} &= (2\pi)^2 h \left(\frac{E_b}{T_b}\right) \overline{p}\left(\frac{m}{K} - \epsilon\right) \qquad (40)
\end{aligned}$$

Substituting Equation (40) into Equation (39) and using Equation (17) leads to the following simplified expression for the symbol timing offset/carrier phase cross term:

$$[\mathbf{F}(\boldsymbol{\theta}|\boldsymbol{\alpha})]_{0,1} = -\frac{2(2\pi)^2 h \rho}{K} \sum_{m=0}^{KL-1} \overline{p}\left(\frac{m}{K} - \epsilon\right) \qquad (41)$$

As with the symbol timing offset/symbol timing offset cross term, we will show in Section VII that the dependency of $[\mathbf{F}(\boldsymbol{\theta}|\boldsymbol{\alpha})]_{0,1}$ in Equation (41) upon ϵ approximately goes away for a periodic preamble waveform $\overline{p}(x)$.

C. Symbol Timing Offset/Carrier Frequency Offset Cross Term

From Equation (30), the symbol timing offset/carrier frequency offset cross term $[\mathbf{F}(\boldsymbol{\theta}|\boldsymbol{\alpha})]_{0,2}$ is given by the following:

$$[\mathbf{F}(\boldsymbol{\theta}|\boldsymbol{\alpha})]_{0,2} = -\frac{2}{\sigma^2}\sum_{m=0}^{KL-1}\mathrm{Re}\left\{s_m^* \cdot \frac{\partial^2 s_m}{\partial\theta_0\partial\theta_2}\right\} \tag{42}$$

Now, using Equations (33) and (31), we have the following set of expressions:

$$\begin{aligned}
\frac{\partial^2 s_m}{\partial\theta_0\partial\theta_2} &= (2\pi)^2 h\left(\frac{m}{K}\right)\overline{p}\left(\frac{m}{K}-\epsilon\right)s_m \\
s_m^* \cdot \frac{\partial^2 s_m}{\partial\theta_0\partial\theta_2} &= (2\pi)^2 h\left(\frac{E_b}{T_b}\right)\left(\frac{m}{K}\right)\overline{p}\left(\frac{m}{K}-\epsilon\right) \\
\mathrm{Re}\left\{s_m^* \cdot \frac{\partial^2 s_m}{\partial\theta_0\partial\theta_2}\right\} &= (2\pi)^2 h\left(\frac{E_b}{T_b}\right)\left(\frac{m}{K}\right)\overline{p}\left(\frac{m}{K}-\epsilon\right)
\end{aligned} \tag{43}$$

Substituting Equation (43) into Equation (42) and using Equation (17) leads to the following simplification for the symbol timing offset/carrier frequency offset cross term:

$$[\mathbf{F}(\boldsymbol{\theta}|\boldsymbol{\alpha})]_{0,2} = -\frac{2(2\pi)^2 h\rho}{K^2}\sum_{m=0}^{KL-1} m\,\overline{p}\left(\frac{m}{K}-\epsilon\right) \tag{44}$$

Unlike the symbol timing offset/symbol timing offset and symbol timing offset/carrier phase cross terms, it is difficult to show that the dependency of $[\mathbf{F}(\boldsymbol{\theta}|\boldsymbol{\alpha})]_{0,2}$ in Equation (44) upon ϵ approximately goes away for a periodic preamble $\overline{p}(x)$. However, in Section VIII, we show that this indeed is approximately true for a worst case value of ϵ. This then suggests that estimation of the symbol timing offset is approximately decoupled from that of the carrier frequency offset.

D. Carrier Phase/Carrier Phase Cross Term

From Equation (30), the carrier phase/carrier phase cross term $[\mathbf{F}(\boldsymbol{\theta}|\boldsymbol{\alpha})]_{1,1}$ is given by

$$[\mathbf{F}(\boldsymbol{\theta}|\boldsymbol{\alpha})]_{1,1} = -\frac{2}{\sigma^2}\sum_{m=0}^{KL-1}\mathrm{Re}\left\{s_m^* \cdot \frac{\partial^2 s_m}{\partial\theta_1^2}\right\} \tag{45}$$

Now, using Equation (32), we have the following set of expressions:

$$\begin{aligned}
\frac{\partial^2 s_m}{\partial\theta_1^2} &= -(2\pi)^2 s_m \\
s_m^* \cdot \frac{\partial^2 s_m}{\partial\theta_1^2} &= -(2\pi)^2\left(\frac{E_b}{T_b}\right) \\
\mathrm{Re}\left\{s_m^* \cdot \frac{\partial^2 s_m}{\partial\theta_1^2}\right\} &= -(2\pi)^2\left(\frac{E_b}{T_b}\right) \\
\sum_{m=0}^{KL-1}\mathrm{Re}\left\{s_m^* \cdot \frac{\partial^2 s_m}{\partial\theta_1^2}\right\} &= -(2\pi)^2\left(\frac{E_b}{T_b}\right)\sum_{m=0}^{KL-1} 1 = -(2\pi)^2\left(\frac{E_b}{T_b}\right)KL
\end{aligned} \tag{46}$$

For the last equality of Equation (46), we used the fact that [13]

$$\sum_{m=0}^{N-1} 1 = N$$

for any $N \in \mathbb{N}^+$. Substituting Equation (46) into Equation (45) and using Equation (17) leads to the following simplified expression for the carrier phase/carrier phase cross term:

$$[\mathbf{F}(\boldsymbol{\theta}|\boldsymbol{\alpha})]_{1,1} = 2(2\pi)^2 L\rho \tag{47}$$

As can be seen from Equation (47), the carrier phase/carrier phase cross term is independent of the preamble waveform $\overline{p}(x)$ and thus the ternary symbol stream $\boldsymbol{\alpha}$.

E. Carrier Phase/Carrier Frequency Offset Cross Term

From Equation (30), the carrier phase/carrier frequency offset cross term $[\mathbf{F}(\boldsymbol{\theta}|\boldsymbol{\alpha})]_{1,2}$ is given by the following:

$$[\mathbf{F}(\boldsymbol{\theta}|\boldsymbol{\alpha})]_{1,2} = -\frac{2}{\sigma^2} \sum_{m=0}^{KL-1} \mathrm{Re}\left\{ s_m^* \cdot \frac{\partial^2 s_m}{\partial\theta_1 \partial\theta_2} \right\} \tag{48}$$

Now, using Equations (33) and (32), we have the following set of expressions:

$$\begin{aligned}
\frac{\partial^2 s_m}{\partial\theta_1\partial\theta_2} &= -(2\pi)^2 \left(\frac{m}{K}\right) s_m \\
s_m^* \cdot \frac{\partial^2 s_m}{\partial\theta_1\partial\theta_2} &= -(2\pi)^2 \left(\frac{m}{K}\right)\left(\frac{E_b}{T_b}\right) \\
\mathrm{Re}\left\{ s_m^* \cdot \frac{\partial^2 s_m}{\partial\theta_1\partial\theta_2} \right\} &= -(2\pi)^2 \left(\frac{m}{K}\right)\left(\frac{E_b}{T_b}\right) \\
\sum_{m=0}^{KL-1} \mathrm{Re}\left\{ s_m^* \cdot \frac{\partial^2 s_m}{\partial\theta_1\partial\theta_2} \right\} &= -(2\pi)^2 \left(\frac{1}{K}\right)\left(\frac{E_b}{T_b}\right) \sum_{m=0}^{KL-1} m \\
&= -(2\pi)^2 \left(\frac{E_b}{T_b}\right) \cdot \frac{(KL-1)L}{2}
\end{aligned} \tag{49}$$

In Equation (49), we used the fact that [13]

$$\sum_{m=0}^{N-1} m = \frac{(N-1)N}{2}$$

for any $N \in \mathbb{N}^+$. Substituting Equation (49) into Equation (48) and using Equation (17) leads to the following simplified expression for the carrier phase/carrier frequency offset cross term:

$$[\mathbf{F}(\boldsymbol{\theta}|\boldsymbol{\alpha})]_{1,2} = \frac{(2\pi)^2 (KL-1)L\rho}{K} \tag{50}$$

As with the carrier phase/carrier phase cross term, from Equation (50), it can be seen that the carrier phase/carrier frequency offset cross term is independent of the preamble waveform $\overline{p}(x)$ and hence the ternary symbol stream $\boldsymbol{\alpha}$.

F. Carrier Frequency Offset/Carrier Frequency Offset Cross Term

From Equation (30), the carrier frequency offset/carrier frequency offset cross term $[\mathbf{F}(\boldsymbol{\theta}|\boldsymbol{\alpha})]_{2,2}$ is given by the following:

$$[\mathbf{F}(\boldsymbol{\theta}|\boldsymbol{\alpha})]_{2,2} = -\frac{2}{\sigma^2}\sum_{m=0}^{KL-1}\mathrm{Re}\left\{s_m^* \cdot \frac{\partial^2 s_m}{\partial\theta_2^2}\right\} \tag{51}$$

Now, using Equation (33), we have the following set of expressions:

$$\begin{aligned}
\frac{\partial^2 s_m}{\partial\theta_2^2} &= -(2\pi)^2\left(\frac{m}{K}\right)^2 s_m \\
s_m^* \cdot \frac{\partial^2 s_m}{\partial\theta_2^2} &= -(2\pi)^2\left(\frac{m}{K}\right)^2\left(\frac{E_b}{T_b}\right) \\
\mathrm{Re}\left\{s_m^* \cdot \frac{\partial^2 s_m}{\partial\theta_2^2}\right\} &= -(2\pi)^2\left(\frac{m}{K}\right)^2\left(\frac{E_b}{T_b}\right) \\
\sum_{m=0}^{KL-1}\mathrm{Re}\left\{s_m^* \cdot \frac{\partial^2 s_m}{\partial\theta_2^2}\right\} &= -(2\pi)^2\left(\frac{1}{K^2}\right)\left(\frac{E_b}{T_b}\right)\sum_{m=0}^{KL-1} m^2 \\
&= -(2\pi)^2\left(\frac{E_b}{T_b}\right)\cdot\frac{(KL-1)(2KL-1)L}{6K}
\end{aligned} \tag{52}$$

In Equation (52), we used the fact that [13]

$$\sum_{m=0}^{N-1} m^2 = \frac{(N-1)N(2N-1)}{6} \tag{53}$$

for any $N \in \mathbb{N}^+$. Substituting Equation (52) into Equation (51) and using Equation (17) leads to the following simplified expression for the carrier frequency offset/carrier frequency offset cross term:

$$[\mathbf{F}(\boldsymbol{\theta}|\boldsymbol{\alpha})]_{2,2} = \frac{(2\pi)^2(KL-1)(2KL-1)L\rho}{3K^2} \tag{54}$$

As with the carrier phase/carrier phase and carrier phase/carrier frequency offset cross terms, from Equation (54), it can be seen that the carrier frequency offset/carrier frequency offset cross term is independent of the preamble waveform $\overline{p}(x)$ and thus the ternary symbol stream $\boldsymbol{\alpha}$.

G. Summary of Results for the Conditional FIM for SOQPSK

Combining all of the results of the previous subsections, it follows that the conditional FIM $\mathbf{F}(\boldsymbol{\theta}|\boldsymbol{\alpha})$ for the SOQPSK signal model of Equation (13) is of the following form:

$$\mathbf{F}(\boldsymbol{\theta}|\boldsymbol{\alpha}) = \begin{bmatrix} F(\epsilon|\boldsymbol{\alpha}) & \mathbf{f}^T(\epsilon|\boldsymbol{\alpha}) \\ \mathbf{f}(\epsilon|\boldsymbol{\alpha}) & \mathbf{A} \end{bmatrix} \tag{55}$$

Here, we have

$$F(\epsilon|\boldsymbol{\alpha}) \triangleq \frac{2(2\pi h)^2\rho}{K}\sum_{m=0}^{KL-1}\overline{p}^2\left(\frac{m}{K}-\epsilon\right) \tag{56}$$

$$\mathbf{f}(\epsilon|\boldsymbol{\alpha}) \triangleq \begin{bmatrix} -\dfrac{2(2\pi)^2 h\rho}{K} \displaystyle\sum_{m=0}^{KL-1} \overline{p}\left(\frac{m}{K} - \epsilon\right) \\ -\dfrac{2(2\pi)^2 h\rho}{K^2} \displaystyle\sum_{m=0}^{KL-1} m\,\overline{p}\left(\frac{m}{K} - \epsilon\right) \end{bmatrix} \tag{57}$$

$$\mathbf{A} \triangleq \begin{bmatrix} 2(2\pi)^2 L\rho & \dfrac{(2\pi)^2(KL-1)L\rho}{K} \\ \dfrac{(2\pi)^2(KL-1)L\rho}{K} & \dfrac{(2\pi)^2(KL-1)(2KL-1)L\rho}{3K^2} \end{bmatrix} \tag{58}$$

From Equations (55) and (58), it can be seen that the lower 2×2 submatrix of $\mathbf{F}(\boldsymbol{\theta}|\boldsymbol{\alpha})$ does not depend upon either the parameter vector $\boldsymbol{\theta}$ or the ternary symbol stream $\boldsymbol{\alpha}$. This will simplify the subsequent derivation of the average FIM in the next section.

VI. Derivation of the Average FIM

Recall from Equation (23) that the average FIM $\mathbf{G}(\boldsymbol{\theta})$ is simply the average of the conditional FIM $\mathbf{F}(\boldsymbol{\theta}|\boldsymbol{\alpha})$ over all possible ternary symbol stream values $\boldsymbol{\alpha}$. From Equation (55), it follows that calculating the average FIM only involves averaging the quantities $F(\epsilon|\boldsymbol{\alpha})$ and $\mathbf{f}(\epsilon|\boldsymbol{\alpha})$ from Equations (56) and (57), respectively, over all possible ternary symbol streams.

A. Symbol Timing Offset/Symbol Timing Offset Cross Term

Consider first the scalar quantity $F(\epsilon|\boldsymbol{\alpha})$ from Equation (56). Using Equation (8) in Equation (56) leads to the following expression:

$$E_{\boldsymbol{\alpha}}\left[F(\epsilon|\boldsymbol{\alpha})\right] = \frac{2(2\pi h)^2\rho}{K} \sum_{m=0}^{KL-1} \sum_{k_0\in\mathbb{Z}} \sum_{k_1\in\mathbb{Z}} E_{\boldsymbol{\alpha}}\left[\alpha_{k_0}\alpha_{k_1}\right] \overline{f}\left(\frac{m}{K} - \epsilon - k_0\right) \overline{f}\left(\frac{m}{K} - \epsilon - k_1\right) \tag{59}$$

For the ternary symbol stream mapping of Equation (3), assuming the serial bit stream is an independent, identically distributed (i.i.d.) sequence [10], we have [4]

$$E_{\boldsymbol{\alpha}}[\alpha_{k_0}\alpha_{k_1}] = R_{\alpha\alpha}[k_0 - k_1] \tag{60}$$

where $R_{\alpha\alpha}[\ell]$ is the autocorrelation function of the ternary symbol stream which satisfies the following relationship [14]:

$$R_{\alpha\alpha}[\ell] = \begin{cases} \frac{1}{2}\,, & \ell = 0 \\ \frac{1}{4}\,, & \ell = \pm 1 \\ 0\,, & \text{otherwise} \end{cases} \tag{61}$$

Using Equations (61) and (60) in Equation (59) yields the following:

$$E_{\boldsymbol{\alpha}}\left[F(\epsilon|\boldsymbol{\alpha})\right] = \frac{2(2\pi h)^2\rho}{K} \sum_{m=0}^{KL-1} \overline{v}\left(\frac{m}{K} - \epsilon\right) \tag{62}$$

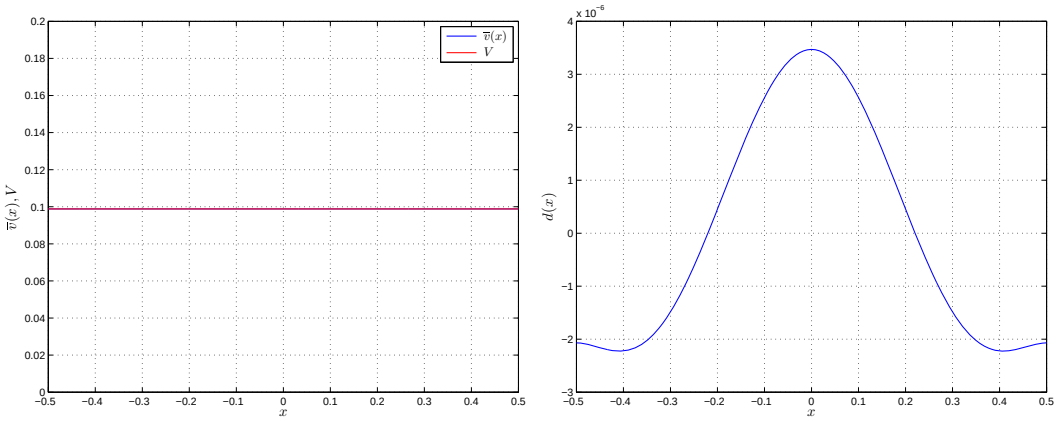

(a) (b)

Figure 2. MCRB dilated pulse function plots: (a) exact pulse waveform $\overline{v}(x)$ overlaid with its approximation V and (b) the difference waveform $d(x) \triangleq \overline{v}(x) - V$.

Here, $\overline{v}(x)$ is the following dilated pulse function:

$$\overline{v}(x) \triangleq \sum_{k\in\mathbb{Z}} \left[\frac{1}{4}\overline{f}(x-k)\overline{f}(x-(k-1)) + \frac{1}{2}\overline{f}^2(x-k) + \frac{1}{4}\overline{f}(x-k)\overline{f}(x-(k+1)) \right] \tag{63}$$

Expressing Equation (63) as three separate summations and then using dummy index variable manipulations, we can simplify the expression for $\overline{v}(x)$ as follows:

$$\overline{v}(x) = \frac{1}{2}\sum_{k\in\mathbb{Z}} \overline{f}(x-k)\left[\overline{f}(x-k) + \overline{f}(x-(k+1))\right] \tag{64}$$

From Equations (63) or (64), it can be seen that $\overline{v}(x)$ is periodic with period 1. For SOQPSK-TG, it turns out that $\overline{v}(x)$ is approximately *constant*. Specifically, we have

$$\overline{v}(x) \approx V\,, \text{ where } V \approx 0.09881 \tag{65}$$

A plot of $\overline{v}(x)$ overlaid with that of V from Equation (65) over the range $-\frac{1}{2} \le x < \frac{1}{2}$ is shown in Figure 2(a). From this, it can be seen that the constant approximation from Equation (65) is a good fit to the exact dilated pulse from Equation (63) or Equation (64). In Figure 2(b), we have plotted the difference signal $d(x) \triangleq \overline{v}(x) - V$, from which it can be seen that the difference is small and less than 3.5×10^{-6}.

Substituting the constant approximation of Equation (65) into Equation (62) yields the following simplified expression for $E_{\boldsymbol{\alpha}}\left[F(\epsilon|\boldsymbol{\alpha})\right]$:

$$E_{\boldsymbol{\alpha}}\left[F(\epsilon|\boldsymbol{\alpha})\right] \approx 2(2\pi h)^2 V L \rho \tag{66}$$

As can be seen from Equation (66), the average FIM symbol timing offset/symbol timing offset cross term approximately does not depend upon any specific value of the parameter vector $\boldsymbol{\theta}$.

B. Symbol Timing Offset/Carrier Phase and Carrier Frequency Offset Cross Terms

Consider now the vector quantity $\mathbf{f}(\epsilon|\boldsymbol{\alpha})$ from Equation (57). Using Equation (8) in Equation (57) leads to the following expression:

$$E_{\boldsymbol{\alpha}}\left[\mathbf{f}(\epsilon|\boldsymbol{\alpha})\right] = \begin{bmatrix} -\dfrac{2(2\pi)^2 h\rho}{K} \displaystyle\sum_{m=0}^{KL-1} \sum_{k\in\mathbb{Z}} E_{\boldsymbol{\alpha}}\left[\alpha_k\right] \overline{f}\left(\dfrac{m}{K} - \epsilon - k\right) \\ -\dfrac{2(2\pi)^2 h\rho}{K^2} \displaystyle\sum_{m=0}^{KL-1} m \sum_{k\in\mathbb{Z}} E_{\boldsymbol{\alpha}}\left[\alpha_k\right] \overline{f}\left(\dfrac{m}{K} - \epsilon - k\right) \end{bmatrix} \tag{67}$$

From the ternary symbol stream mapping given in Equation (3), for an i.i.d. serial bit stream $\{b_k\}$, we have $E_{\boldsymbol{\alpha}}\left[\alpha_k\right] = 0$ for all k and so Equation (67) simplifies to the following:

$$E_{\boldsymbol{\alpha}}\left[\mathbf{f}(\epsilon|\boldsymbol{\alpha})\right] = \begin{bmatrix} 0 \\ 0 \end{bmatrix} = \mathbf{0} \tag{68}$$

As the symbol timing offset/carrier phase and carrier frequency offset cross terms are zero from Equation (68), this implies that in terms of the MCRB, the symbol timing offset is completely decoupled from the carrier phase and carrier frequency offset. In other words, estimating the symbol timing offset has no effect on estimating either the carrier phase or carrier frequency offset and vice versa.

C. Summary of Results for the Average FIM for SOQPSK

Substituting Equations (66) and (68) in Equations (23) and (55) leads to the following approximation for the average FIM $\mathbf{G}(\boldsymbol{\theta})$:

$$\mathbf{G}(\boldsymbol{\theta}) \approx \begin{bmatrix} 2(2\pi h)^2 VL\rho & \mathbf{0} \\ \mathbf{0} & \mathbf{A} \end{bmatrix} \tag{69}$$

Here, $\mathbf{A}$ is the matrix given in Equation (58). Upon further inspection of Equations (69) and (58), it follows that $\mathbf{G}(\boldsymbol{\theta})$ can be further simplified to the following approximation:

$$\mathbf{G}(\boldsymbol{\theta}) \approx \begin{bmatrix} 2h^2 V & 0 & 0 \\ 0 & 2 & \frac{KL-1}{K} \\ 0 & \frac{KL-1}{K} & \frac{(KL-1)(2KL-1)}{3K^2} \end{bmatrix} (2\pi)^2 L\rho \tag{70}$$

From Equation (70), it can be seen that the average FIM is a linear function of the bit SNR ρ. As such, from Equation (21), it follows that the MCRB is linearly inversely proportional to the bit SNR.

VII. Simplification of the Conditional FIM for Periodic Preamble Waveforms

Prior to incorporating a periodic constraint on the preamble waveform $\overline{p}(x)$ to simplify the conditional FIM terms $F(\epsilon|\boldsymbol{\alpha})$ and $\mathbf{f}(\epsilon|\boldsymbol{\alpha})$ from Equations (56) and (57), respectively, it is

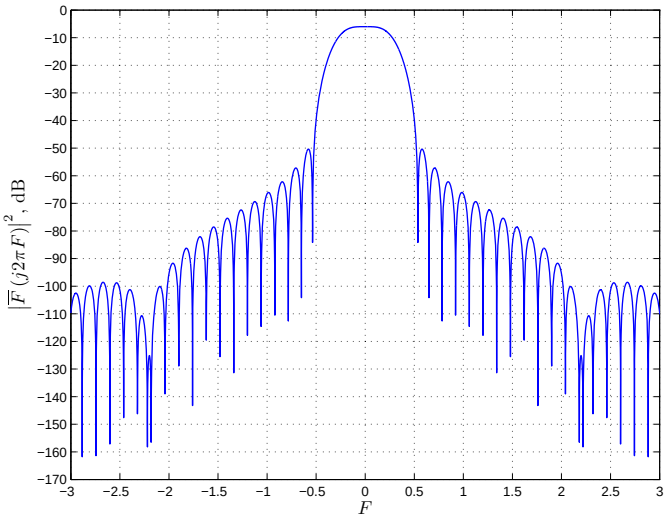

Figure 3. Plot of the magnitude response of $\overline{F}(j2\pi F)$ on a dB scale.

worthwhile investigating other inherent properties of $\overline{p}(x)$ for SOQPSK-TG specifically. To that end, recall that $\overline{p}(x)$ is given by Equation (8), where $\overline{f}(x)$ is the dilated frequency pulse function, which for SOQPSK-TG is as plotted in Figure 1. Taking the Fourier transform [8, 9] of both sides of Equation (8) yields the following:

$$\overline{P}(j2\pi F) = \overline{F}(j2\pi F)A(e^{j2\pi F}) \tag{71}$$

Here, $\overline{P}(j2\pi F)$ and $\overline{F}(j2\pi F)$ denote, respectively, the continuous-time Fourier transforms [8, 9] of $\overline{p}(x)$ and $\overline{f}(x)$, and $A(e^{j2\pi f})$ denotes the discrete-time Fourier transform [8, 9] of the ternary symbol sequence $\{\alpha_k\}$ given by

$$A(e^{j2\pi f}) = \sum_{k\in\mathbb{Z}} \alpha_k e^{-j2\pi fk}$$

From Equation (71), it is clear that $\overline{P}(j2\pi F)$ is the product of a periodic function $A(e^{j2\pi F})$ (with period 1) and an aperiodic function $\overline{F}(j2\pi F)$. For SOQPSK-TG, we will argue that $\overline{P}(j2\pi F)$ is approximately bandlimited to the region $F \in [-1/2, 1/2)$. To show this, we have plotted the magnitude of $\overline{F}(j2\pi F)$ on a dB scale in Figure 3.

As can be seen from Figure 3, the majority of the energy of $\overline{F}(j2\pi F)$ is concentrated in the region $F \in [-1/2, 1/2)$. Multiplying $\overline{F}(j2\pi F)$ by the periodic function $A(e^{j2\pi F})$ will not widen this energy distribution and thus $\overline{P}(j2\pi F)$ is approximately bandlimited to $F \in [-1/2, 1/2)$.

Let us now incorporate a periodic constraint on $\overline{p}(x)$. From Equation (8), it can be seen that $\overline{p}(x)$ can be periodic if and only if the ternary symbol sequence $\{\alpha_k\}$ is periodic. Furthermore, if $\{\alpha_k\}$ is periodic with period P (where we must have $P \in \mathbb{N}^+$), then $\overline{p}(x)$ is also periodic with period P. With the bandlimited approximation in effect, it follows that

$\overline{p}(x)$ has the following Fourier series expansion [8, 9]:

$$\overline{p}(x) = \sum_{k\in\mathbb{Z}} c_k e^{j\frac{2\pi kx}{P}}\,, \text{ where } c_k \text{ is only nonzero for } -\left\lfloor \tfrac{P}{2} \right\rfloor \leq k \leq \left\lceil \tfrac{P}{2} \right\rceil - 1 \tag{72}$$

Here, $\{c_k\}$ denotes the set of Fourier series coefficients of $\overline{p}(x)$ [8, 9]. Throughout the rest of this section, we will assume that $\overline{p}(x)$ is periodic with period $P \in \mathbb{N}^+$ with the expansion given in Equation (72).

Finally, prior to proceeding further with the simplification of the conditional FIM terms dependent upon $\overline{p}(x)$, we will assume that the number of bits observed L from Equation (16) is an integer multiple of the period P. In other words, we will assume that we have

$$L = PM\,, \text{ for some } M \in \mathbb{N}^+ \tag{73}$$

With these assumptions in place, we are now ready to simplify the preamble dependent conditional FIM terms.

A. Symbol Timing Offset/Symbol Timing Offset Cross Term

Consider the conditional FIM term $F(\epsilon|\boldsymbol{\alpha})$ from Equation (56). Let S_0 denote the preamble dependent summation from Equation (56). In other words, define S_0 as follows:

$$S_0 \triangleq \sum_{m=0}^{KL-1} \overline{p}^2\left(\frac{m}{K} - \epsilon\right) = \sum_{m=0}^{KPM-1} \left|\overline{p}\left(\frac{m}{K} - \epsilon\right)\right|^2 \tag{74}$$

Here, the second equality from Equation (74) follows from Equation (73) and the fact that $\overline{p}(x)$ is a real function. Substituting Equation (72) into Equation (74) yields the following expression after some algebraic manipulation:

$$S_0 = \sum_{k_0\in\mathbb{Z}} \sum_{k_1\in\mathbb{Z}} c_{k_0} c_{k_1}^* e^{-j\frac{2\pi(k_0-k_1)\epsilon}{P}} \underbrace{\left(\sum_{m=0}^{PKM-1} e^{j\frac{2\pi(k_0-k_1)m}{PK}}\right)}_{S_g[k_0-k_1]} \tag{75}$$

In Equation (75), $S_g[k]$ denotes a finite geometric series which can be simplified as follows. By the division theorem [9], the dummy variable m in Equation (75) can be decomposed into a quotient and remainder form as shown below:

$$m = (PK)q + r\,,\ 0 \leq q \leq M-1\,, 0 \leq r \leq PK-1 \tag{76}$$

Here, $q \triangleq \left\lfloor \frac{m}{PK} \right\rfloor$ is the *quotient* and $r \triangleq m \bmod (PK)$ is the *remainder* when m is divided by PK. Incorporating Equation (76) into the expression for $S_g[k]$ leads to the following chain of equalities:

$$\begin{aligned} S_g[k] &= \sum_{q=0}^{M-1}\sum_{r=0}^{PK-1} e^{j\frac{2\pi k((PK)q+r)}{PK}} = \sum_{q=0}^{M-1}\sum_{r=0}^{PK-1} e^{j2\pi kq} e^{j\frac{2\pi kr}{PK}} \\ &= \sum_{q=0}^{M-1}\sum_{r=0}^{PK-1} e^{j\frac{2\pi kr}{PK}} = M\sum_{r=0}^{PK-1}\left(e^{\frac{j2\pi k}{PK}}\right)^r \end{aligned} \tag{77}$$

The first equality of Equation (77) follows from the fact that $e^{j2\pi n} = 1$ for any $n \in \mathbb{Z}$. Note that the summation appearing at the end of Equation (77) is simply a finite geometric series over various roots of unity [9] for which we have [13]

$$\sum_{r=0}^{PK-1} \left(e^{\frac{j2\pi k}{PK}}\right)^r = \begin{cases} PK\,, & k \equiv 0 \bmod (PK) \\ 0\,, & k \not\equiv 0 \bmod (PK) \end{cases} \tag{78}$$

Substituting Equation (78) into Equation (77) yields the following:

$$S_g[k] = \begin{cases} MPK\,, & k \equiv 0 \bmod (PK) \\ 0\,, & k \not\equiv 0 \bmod (PK) \end{cases} = \begin{cases} KL\,, & k \equiv 0 \bmod (PK) \\ 0\,, & k \not\equiv 0 \bmod (PK) \end{cases} \tag{79}$$

Upon substituting Equation (79) into Equation (75), it follows that for fixed k_0, by summing over k_1, only the terms for which $k_1 = k_0 - PK\ell$ for any $\ell \in \mathbb{Z}$ are nonzero. Hence, Equation (75) simplifies as follows:

$$S_0 = KL \sum_{k_0 \in \mathbb{Z}} \sum_{\ell \in \mathbb{Z}} c_{k_0} c^*_{k_0 - PK\ell} e^{-j2\pi(K\epsilon)\ell} = KL \sum_{\ell \in \mathbb{Z}} \left\{ \sum_{k_0 \in \mathbb{Z}} c_{k_0} c^*_{k_0 - PK\ell} \right\} e^{-j2\pi(K\epsilon)\ell} \tag{80}$$

Note that the term in braces in Equation (80) is simply a value of the deterministic autocorrelation of the Fourier series coefficients $\{c_k\}$ [8]. In other words, if $R_{cc}[\ell]$ denotes the deterministic autocorrelation of the Fourier series coefficients defined as [8]

$$R_{cc}[\ell] \triangleq \sum_{k=-\infty}^{\infty} c_k c^*_{k-\ell} \tag{81}$$

then the expression in Equation (80) simplifies to the following:

$$S_0 = KL \sum_{\ell \in \mathbb{Z}} R_{cc}[(PK)\ell] e^{-j2\pi(K\epsilon)\ell} \tag{82}$$

From Equation (72), as c_k is only nonzero for $-\left\lfloor \frac{P}{2} \right\rfloor \leq k \leq \left\lceil \frac{P}{2} \right\rceil - 1$, it follows from Equation (81) that $R_{cc}[\ell]$ is only nonzero for $-(P-1) \leq \ell \leq (P-1)$. As such, only the $\ell = 0$ term from Equation (82) survives and S_0 then simplifies to the following expression:

$$S_0 = KLR_{cc}[0] \tag{83}$$

By Parseval's theorem [8], it can be shown that

$$R_{cc}[0] = \sum_{k \in \mathbb{Z}} |c_k|^2 = \frac{1}{P} \int_{x_0}^{x_0+P} |\overline{p}(x)|^2 \, dx = \mathcal{E}_{\overline{p}}(\boldsymbol{\alpha}) \tag{84}$$

for any $x_0 \in \mathbb{R}$, where $\mathcal{E}_{\overline{p}}(\boldsymbol{\alpha})$ denotes the *energy* of the periodic preamble waveform $\overline{p}(x)$. Combining Equations (84), (83), and (56), it follows that the conditional FIM term $F(\epsilon|\boldsymbol{\alpha})$ simplifies to the following expression for a periodic preamble:

$$F(\epsilon|\boldsymbol{\alpha}) = 2(2\pi h)^2 \mathcal{E}_{\overline{p}}(\boldsymbol{\alpha}) L\rho \tag{85}$$

Note the similarities between Equation (85) and Equation (66) which was derived for the average FIM symbol timing offset/symbol timing offset cross term.

B. Symbol Timing Offset/Carrier Phase Cross Term

Consider the symbol timing offset/carrier phase conditional FIM cross term $[\mathbf{f}(\epsilon|\boldsymbol{\alpha})]_0$ from Equation (57). Let S_1 denote the preamble dependent summation from the first component of Equation (57). In other words, define S_1 as follows:

$$S_1 \triangleq \sum_{m=0}^{KL-1} \overline{p}\left(\frac{m}{K} - \epsilon\right) = \sum_{m=0}^{KPM-1} \overline{p}\left(\frac{m}{K} - \epsilon\right) \tag{86}$$

Here, the second equality from Equation (86) results from Equation (73). Substituting Equation (72) into Equation (86) yields the following after some algebraic manipulation:

$$S_1 = \sum_{k\in\mathbb{Z}} c_k e^{-j\frac{2\pi k\epsilon}{P}} \underbrace{\left(\sum_{m=0}^{PKM-1} e^{j\frac{2\pi km}{PK}}\right)}_{S_g[k]} \tag{87}$$

Substituting the expression for $S_g[k]$ from Equation (79), we obtain the following simplified expression for S_1:

$$S_1 = KL \sum_{\ell\in\mathbb{Z}} c_{(PK)\ell} e^{-j2\pi(K\epsilon)\ell} \tag{88}$$

As c_k is only nonzero for $-\left\lfloor\frac{P}{2}\right\rfloor \leq k \leq \left\lceil\frac{P}{2}\right\rceil - 1$ from Equation (72), it follows that only the term $\ell = 0$ from Equation (88) survives and so we have the following:

$$S_1 = KLc_0 \tag{89}$$

Now note that we have [8]

$$c_0 = \frac{1}{P}\int_{x_0}^{x_0+P} \overline{p}(x)\,dx = \mu_{\overline{p}}(\boldsymbol{\alpha}) \tag{90}$$

for any $x_0 \in \mathbb{R}$, where $\mu_{\overline{p}}(\boldsymbol{\alpha})$ denotes the *mean* of the periodic preamble waveform $\overline{p}(x)$. Combining Equations (90), (89), and (57), it follows that the conditional FIM term $[\mathbf{f}(\epsilon|\boldsymbol{\alpha})]_0$ simplifies to the following expression for a periodic preamble:

$$[\mathbf{f}(\epsilon|\boldsymbol{\alpha})]_0 = -2(2\pi)^2 h\mu_{\overline{p}}(\boldsymbol{\alpha})L\rho \tag{91}$$

Note that from Equation (91), the symbol timing offset/carrier phase conditional FIM cross term is approximately independent of the parameter ϵ for a periodic preamble waveform $\overline{p}(x)$.

C. Symbol Timing Offset/Carrier Frequency Offset Cross Term

Consider the symbol timing offset/carrier frequency offset conditional FIM cross term $[\mathbf{f}(\epsilon|\boldsymbol{\alpha})]_1$ from Equation (57). Let S_2 denote the preamble dependent summation from the first component of Equation (57). In other words, define S_2 as follows:

$$S_2 \triangleq \sum_{m=0}^{KL-1} m\overline{p}\left(\frac{m}{K} - \epsilon\right) \tag{92}$$

Unfortunately, it does not appear possible to simplify S_2 in such a way as to eliminate the dependency upon ϵ. However, it is still possible to bound the magnitude of S_2. In order to do this, recall the *Cauchy-Schwarz inequality* [13], which states that for any two complex sequences $\{x_i\}$ and $\{y_i\}$ defined over some index set $\mathcal{I}$, we have the following:

$$\left|\sum_{i\in\mathcal{I}} x_i y_i^*\right|^2 \leq \left(\sum_{i\in\mathcal{I}} |x_i|^2\right)\left(\sum_{i\in\mathcal{I}} |y_i|^2\right) \tag{93}$$

Equality holds in Equation (93) if and only if $y_i = Cx_i$ for all $i \in \mathcal{I}$, where $C \in \mathbb{C}$ is some complex scalar quantity.

Applying Equation (93) to Equation (92) yields the following:

$$\begin{aligned}
|S_2| &\leq \sqrt{\left(\sum_{m=0}^{KL-1} m^2\right)\left(\sum_{m=0}^{KL-1} \overline{p}^2\left(\frac{m}{K}-\epsilon\right)\right)} \\
&= \sqrt{\left(\frac{(KL-1)(KL)(2KL-1)}{6}\right)(S_0)} &(94)\\
&= \sqrt{\frac{(KL-1)(KL)(2KL-1)}{6}\cdot KL\mathcal{E}_{\overline{p}}(\boldsymbol{\alpha})} &(95)\\
&= KL\sqrt{\frac{(KL-1)(2KL-1)}{6}\mathcal{E}_{\overline{p}}(\boldsymbol{\alpha})} &(96)
\end{aligned}$$

Here, Equation (94) follows from Equation (53) and the definition of S_0 given in Equation (74), whereas Equation (95) follows from Equations (83) and (84). It should be noted that while Equation (96) represents a bound on the magnitude of S_2 that is independent of ϵ, it will tend to yield an overly pessimistic bound in practice since the condition for equality, namely $\overline{p}\left(\frac{m}{K}-\epsilon\right) = Cm$ for all $0 \leq m \leq KL-1$, will be far from holding for actual candidate periodic preamble waveforms.

D. Summary of Results for the Conditional FIM for Periodic Preamble Waveforms

Combining the results of this section, we can express the conditional FIM for periodic preamble waveforms in the spirit of Equation (70) as follows:

$$\mathbf{F}(\boldsymbol{\theta}|\boldsymbol{\alpha}) \approx \begin{bmatrix} 2h^2\mathcal{E}_{\overline{p}}(\boldsymbol{\alpha}) & -2h\mu_{\overline{p}}(\boldsymbol{\alpha}) & T(\epsilon|\boldsymbol{\alpha}) \\ -2h\mu_{\overline{p}}(\boldsymbol{\alpha}) & 2 & \frac{KL-1}{K} \\ T(\epsilon|\boldsymbol{\alpha}) & \frac{KL-1}{K} & \frac{(KL-1)(2KL-1)}{3K^2} \end{bmatrix}(2\pi)^2 L\rho \tag{97}$$

Here, $T(\epsilon|\boldsymbol{\alpha})$ is defined as follows:

$$T(\epsilon|\boldsymbol{\alpha}) \triangleq -\frac{2h}{K}\left[\frac{1}{KL}\sum_{m=0}^{KL-1} m\overline{p}\left(\frac{m}{K}-\epsilon\right)\right] \tag{98}$$

Note that $T(\epsilon|\boldsymbol{\alpha})$ as defined in Equation (98) is independent of the bit SNR ρ. As such, from Equation (97), it can be seen that the conditional FIM is a linear function of the bit SNR and thus the CCRB is linearly inversely proportional to the bit SNR.

VIII. Performance Bounds for Candidate Periodic Preambles for SOQPSK-TG

Intuitively, for a fixed bit SNR, we wish to select preamble waveforms that will yield the lowest possible mean squared error (MSE) for the parameters to be estimated. One way to attempt to do this is by *decoupling* the parameters as best as possible in this setting [15]. In other words, we want to minimize the effect that estimating a given parameter has on estimating any of the other parameters, as any error made in estimating a given parameter will tend to have a deleterious effect on estimating the other parameters. This can be accomplished here by making the FIM as *diagonally dominant* as possible.

From the expression for the conditional FIM given in Equation (97) for periodic preamble waveforms, it can be seen that the FIM can be made diagonally dominant by maximizing the energy $\mathcal{E}_{\overline{p}}(\boldsymbol{\alpha})$ and minimizing the magnitude of the mean $|\mu_{\overline{p}}(\boldsymbol{\alpha})|$. As such, we will focus on zero-mean preambles with maximal energy.

The choice of the ternary symbol sequence $\{\alpha_k\}$ used to generate a given preamble is constrained by the relation given in Equation (3). This relation leads to a four-state time-varying trellis [10] used to generate the sequence $\{\alpha_k\}$ which imposes constraints on the allowable transitions of the ternary data [11]. For example, a value of $\alpha_k = 1$ cannot be followed by $\alpha_{k+1} = -1$ and vice versa [11].

To maximize the energy of a periodic preamble waveform for a given period length P, we wish to maximize the number of consecutive $+1$s or -1s. The reason for this is to minimize the destructive interference caused by the sidelobes (see Figure 1) of shifted copies of the dilated frequency pulse $\overline{f}(x)$ from Equation (8). To make the preamble zero-mean, we need the number of $+1$s to equal the number of -1s. Due to the above mentioned constraint on the ternary data, a string of $+1$s cannot be immediately followed by a string of -1s. In this case, in order to maximize the energy while making the preamble zero-mean, a string of $+1$s (or -1s) will be separated by a string of -1s (or $+1$s) by a single 0.

For example, suppose the period P is 4, 8, and 16. Using the preamble construction approach advocated above, this leads to the following ternary symbol stream values for each period length:

$$P = 4 \implies \{\alpha_k\} = \{\ldots, 1, 0, -1, 0, \ldots\} \tag{99}$$

$$P = 8 \implies \{\alpha_k\} = \{\ldots, \underbrace{1, 1, 1}_{3\ +1\text{s}}, 0, \underbrace{-1, -1, -1}_{3\ -1\text{s}}, 0, \ldots\} \tag{100}$$

$$P = 16 \implies \{\alpha_k\} = \{\ldots, \underbrace{1, 1, 1, 1, 1, 1, 1}_{7\ +1\text{s}}, 0, \underbrace{-1, -1, -1, -1, -1, -1, -1}_{7\ -1\text{s}}, 0, \ldots\} \tag{101}$$

For the periodic preambles described by Equations (99), (100), and (101), we calculated the CCRB as a function of the bit SNR ρ for SOQPSK-TG. To conform to the iNET 128-bit preamble length, we opted to consider $L = 128$. Here, an oversampling factor of $K = 4$ was selected. In addition to the CCRB, the MCRB was also computed. Plots of the resulting MSEs for each parameter are shown in Figure 4 for (a) the normalized symbol timing offset, (b) the normalized carrier phase, and (c) the normalized carrier frequency

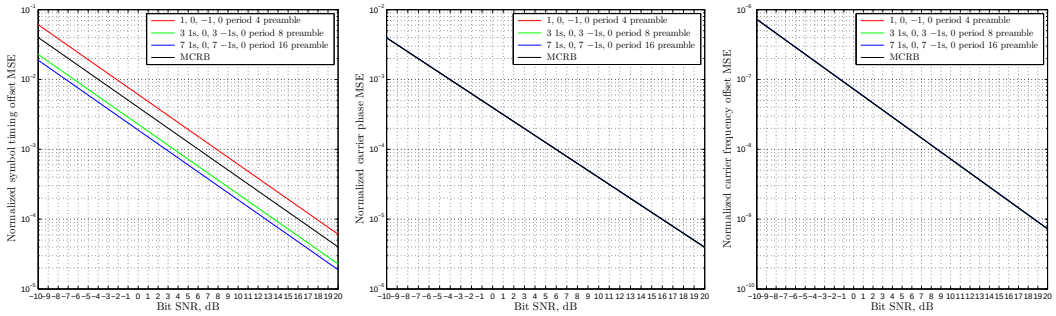

(a) (b) (c)

Figure 4. MSE plots as a function of bit SNR: (a) normalized symbol timing offset, (b) normalized carrier phase, and (c) normalized carrier frequency offset.

offset. It should be noted here that for each candidate preamble, $T(\epsilon|\boldsymbol{\alpha})$ from Equation (98) was calculated for all possible ϵ and the value selected for the plots here was the one which yielded the largest magnitude for $T(\epsilon|\boldsymbol{\alpha})$ as this can be shown to yield the largest degradation in terms of overall MSE [15].

As can be seen from Figure 4, the candidate preambles affect the normalized symbol timing offset MSE performance but appear to not have any effect on the performance of the normalized carrier phase and carrier frequency offset MSEs. This suggests that for the candidate preambles considered, estimation of the symbol timing is approximately decoupled from the estimation of the carrier phase and carrier frequency offset, as desired.

A closer inspection of the carrier phase and carrier frequency offset MSEs reveals that there is some minute coupling effect still in place, however. In Figure 5, we have showed zoomed in plots of the MSE for (a) the normalized carrier phase and (b) the normalized carrier frequency offset. As can be seen, the better a preamble performs in terms of symbol timing MSE, the worse it performs in terms of carrier phase and carrier frequency offset MSE. Despite this phenomenon, it can be seen that the penalty is small and less than 0.05 dB bit SNR for both cases.

Returning our attention to Figure 4(a), it can be seen that the candidate preambles yield increasingly improved performance as the period increases. This is due to the fact that as the period increases, the energy of the preamble increases relative to the energy lost due to the transition from the string of $+1$s to the string of -1s. Note that the period-4 preamble from Equation (99) yielded worse performance than the MCRB, while all other candidate preambles considered yielded superior performance. Since the MCRB approximately represents a warped average of the performance of all possible preambles, this means that the period-4 preamble is performing *worse* than average, while all other candidate preambles are performing *better* than average.

As a result of this, the period-4 preamble is not a suitable one to use in practice for symbol timing acquisition. This observation is particularly interesting as the period-4

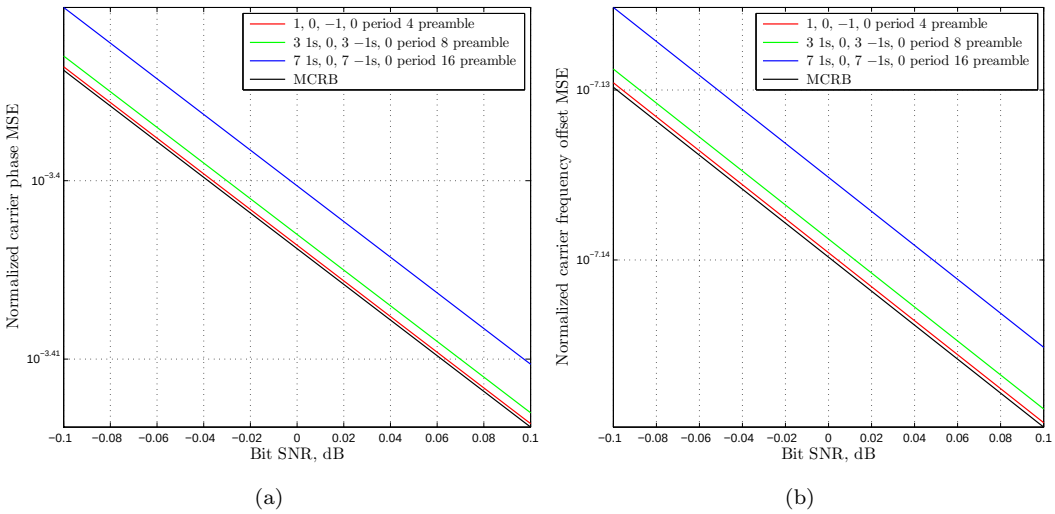

Figure 5. Zoomed in MSE plots as a function of bit SNR: (a) normalized carrier phase and (b) normalized carrier frequency offset.

preamble of Equation (99) is the one used for MIL-STD-188-181A SOQPSK for acquisition [16]. While this preamble is well suited for MIL-STD-188-181A SOQPSK, which uses a rectangular shaped full response frequency pulse, it is not well suited for SOQPSK-TG, which uses the partial response frequency pulse shown in Figure 1. The reason for this is that the partial response sidelobes of the SOQPSK-TG frequency pulse cause destructive interference in the preamble, while the MIL-STD-188-181A SOQPSK full response frequency pulse incurs no such interference for its preamble waveform.

IX. Concluding Remarks

In this paper, we derived performance bounds for the joint estimation of the symbol timing, carrier phase, and carrier frequency offset of a sampled SOQPSK waveform corrupted by noise. Here, in addition to calculating the preamble dependent conditional FIM (used to compute the CCRB), we also calculated the preamble independent average FIM (used to calculate the MCRB). Furthermore, we showed how to simplify the conditional FIM for periodic preamble waveforms. For SOQPSK-TG, MSE simulation results for a set of candidate periodic preambles were provided showing the benefits and risks associated with each preamble with respect to the MCRB. It was shown that significant improvement in symbol timing estimation performance could be obtained with negligible degradation with respect to carrier phase and carrier frequency offset estimation.

The analysis provided herein could be used to stipulate a preamble sequence to use for the iNET burst preamble [1]. However, the final selection of a preamble should not only be based upon its parameter estimation MSE performance, but upon other factors as well. Specifically, spectral mask conformance and computational complexity for acquisition should also be taken into account when selecting a preamble sequence.

References

[1] integrated Network Enhanced Telemetry (iNET) Communication Link Standard Working Group, *Communication Link Standard*, Proposed Version 0.7, Central Test and Evaluation Investment Program (CTEIP), Jan. 31, 2010.

[2] T. J. Hill, "A Non-Proprietary, Constant Envelope, Variant of Shaped Offset QPSK (SOQPSK) for Improved Spectral Containment and Detection Efficiency," in *Proceedings of the 21st Century Military Communications Conference (MILCOM 2000)*, vol. 1, Los Angeles, California, USA, Oct. 22–25, 2000, pp. 347–352.

[3] E. Perrins and M. Rice, "Reduced-Complexity Approach to Iterative Detection of Coded SOQPSK," *IEEE Transactions on Communications*, vol. 55, no. 7, pp. 1354–1362, Jul. 2007.

[4] P. Chandran and E. Perrins, "Decision Directed Timing Recovery for SOQPSK," in *Proceedings of the IEEE Military Communications Conference (MILCOM 2007)*, Orlando, Florida, USA, Oct. 29–31, 2007, pp. 1–6.

[5] C. W. Therrien, *Discrete Random Signals and Statistical Signal Processing*. Upper Saddle River, NJ: Prentice-Hall, Inc., 1992.

[6] A. N. D'Andrea, U. Mengali, and R. Reggiannini, "The Modified Cramer-Rao Bound and its Application to Synchronization Problems," *IEEE Transactions on Communications*, vol. 42, no. 2/3/4, pp. 1391–1399, Feb./Mar./Apr. 1994.

[7] U. Mengali and A. N. D'Andrea, *Synchronization Techniques for Digital Receivers*. New York, NY: Kluwer Academic/Plenum Publishers, 1997.

[8] A. V. Oppenheim and R. W. Schafer, *Discrete-Time Signal Processing*, 3rd ed. Upper Saddle River, NJ: Prentice-Hall, Inc., 2009.

[9] P. P. Vaidyanathan, *Multirate Systems and Filter Banks*. Englewood Cliffs, NJ: Prentice Hall PTR, 1993.

[10] M. K. Simon, S. M. Hinedi, and W. C. Lindsey, *Digital Communications Techniques: Signal Design and Detection*. Upper Saddle River, NJ: Prentice Hall PTR, 1994.

[11] E. Perrins, R. Schober, M. Rice, and M. K. Simon, "Multiple-Bit Differential Detection of Shaped-Offset QPSK," *IEEE Transactions on Communications*, vol. 55, no. 12, pp. 2328–2340, Dec. 2007.

[12] R. A. Horn and C. R. Johnson, *Matrix Analysis*. Cambridge, UK: Cambridge University Press, 1985.

[13] I. S. Gradshteyn and I. M. Ryzhik, *Table of Integrals, Series, and Products*, 6th ed. San Diego, CA: Academic Press, 2000.

[14] M. K. Simon, "Multiple-Bit Differential Detection of Offset QPSK," *IEEE Transactions on Communications*, vol. 51, no. 6, pp. 1004–1011, Jun. 2003.

[15] G. N. Tavares and L. M. Tavares, "Sequence Design for Data-Aided Estimation of Synchronization Parameters," *IEEE Transactions on Communications*, vol. 55, no. 4, pp. 670–677, Apr. 2007.

[16] Defense Information Systems Agency, *Interoperability Standard for Single-Access 5-kHz and 25-kHz UHF Satellite Communications*, Department of Defense Std., Rev. MIL-STD-188-181A, Mar. 31, 1997.

Appendix: Relationship Between the Unconditional and Modified CRBs

In this section, we prove the matrix inequality from Equation (27). To prove this relation, it suffices to prove the following statement:

$$\mathbf{G}(\boldsymbol{\theta}) \geq \mathbf{H}(\boldsymbol{\theta}) \tag{A-1}$$

Here, $\mathbf{G}(\boldsymbol{\theta})$ and $\mathbf{H}(\boldsymbol{\theta})$ are the average and unconditional FIMs given by Equations (22) and (25), respectively. The reason that Equation (27) follows from Equation (A-1) is due to the fact that if $\mathbf{A}$ and $\mathbf{B}$ are positive definite with $\mathbf{A} \geq \mathbf{B}$, then we have $\mathbf{B}^{-1} \geq \mathbf{A}^{-1}$ [12]:

To prove Equation (A-1), it is convenient to define the conditional and unconditional *scores* [5]. These vectors are respectively defined as follows:

$$\mathbf{s}(\mathbf{y}|\boldsymbol{\alpha};\boldsymbol{\theta}) \triangleq \nabla_{\boldsymbol{\theta}} \ln p(\mathbf{y}|\boldsymbol{\alpha};\boldsymbol{\theta}) \tag{A-2}$$

$$\mathbf{s}(\mathbf{y};\boldsymbol{\theta}) \triangleq \nabla_{\boldsymbol{\theta}} \ln p(\mathbf{y};\boldsymbol{\theta}) \tag{A-3}$$

The conditional and unconditional FIMs $\mathbf{G}(\boldsymbol{\theta})$ and $\mathbf{H}(\boldsymbol{\theta})$ can be expressed in terms of the scores as follows [5]:

$$\mathbf{G}(\boldsymbol{\theta}) = E_{\mathbf{y},\boldsymbol{\alpha}}\left[\mathbf{s}(\mathbf{y}|\boldsymbol{\alpha};\boldsymbol{\theta})\mathbf{s}^T(\mathbf{y}|\boldsymbol{\alpha};\boldsymbol{\theta})\right] = E_{\mathbf{y},\boldsymbol{\alpha}}\left[\mathbf{s}(\mathbf{y}|\boldsymbol{\alpha};\boldsymbol{\theta})\mathbf{s}^\dagger(\mathbf{y}|\boldsymbol{\alpha};\boldsymbol{\theta})\right] \tag{A-4}$$

$$\mathbf{H}(\boldsymbol{\theta}) = E_{\mathbf{y}}\left[\mathbf{s}(\mathbf{y};\boldsymbol{\theta})\mathbf{s}^T(\mathbf{y};\boldsymbol{\theta})\right] = E_{\mathbf{y}}\left[\mathbf{s}(\mathbf{y};\boldsymbol{\theta})\mathbf{s}^\dagger(\mathbf{y};\boldsymbol{\theta})\right] \tag{A-5}$$

Let us now define $\mathbf{K}(\boldsymbol{\theta})$ to be the following autocorrelation matrix:

$$\mathbf{K}(\boldsymbol{\theta}) \triangleq E_{\mathbf{y},\boldsymbol{\alpha}}\left[\left(\mathbf{s}(\mathbf{y}|\boldsymbol{\alpha};\boldsymbol{\theta}) - \mathbf{s}(\mathbf{y};\boldsymbol{\theta})\right)\left(\mathbf{s}(\mathbf{y}|\boldsymbol{\alpha};\boldsymbol{\theta}) - \mathbf{s}(\mathbf{y};\boldsymbol{\theta})\right)^\dagger\right] \tag{A-6}$$

From this, it is clear that $\mathbf{K}(\boldsymbol{\theta}) \geq \mathbf{0}$ with equality if and only if $\mathbf{s}(\mathbf{y}|\boldsymbol{\alpha};\boldsymbol{\theta}) = \mathbf{s}(\mathbf{y};\boldsymbol{\theta})$ [12]. Expanding Equation (A-6) and using Equations (A-5) and (A-4), we have

$$\mathbf{K}(\boldsymbol{\theta}) = \mathbf{G}(\boldsymbol{\theta}) - E_{\mathbf{y},\boldsymbol{\alpha}}\left[\mathbf{s}(\mathbf{y}|\boldsymbol{\alpha};\boldsymbol{\theta})\mathbf{s}^\dagger(\mathbf{y};\boldsymbol{\theta})\right] - E_{\mathbf{y},\boldsymbol{\alpha}}\left[\mathbf{s}(\mathbf{y};\boldsymbol{\theta})\mathbf{s}^\dagger(\mathbf{y}|\boldsymbol{\alpha};\boldsymbol{\theta})\right] + \mathbf{H}(\boldsymbol{\theta}) \tag{A-7}$$

To simplify the cross terms in Equation (A-7), consider the first one. Note that we have the following here:

$$E_{\mathbf{y},\boldsymbol{\alpha}}\left[\mathbf{s}(\mathbf{y}|\boldsymbol{\alpha};\boldsymbol{\theta})\mathbf{s}^\dagger(\mathbf{y};\boldsymbol{\theta})\right] = E_{\mathbf{y}}\left\{E_{\boldsymbol{\alpha}|\mathbf{y}}\left[\mathbf{s}(\mathbf{y}|\boldsymbol{\alpha};\boldsymbol{\theta})\mathbf{s}^\dagger(\mathbf{y};\boldsymbol{\theta})\right]\right\} \tag{A-8}$$

$$= E_{\mathbf{y}}\left\{\left(E_{\boldsymbol{\alpha}|\mathbf{y}}\left[\mathbf{s}(\mathbf{y}|\boldsymbol{\alpha};\boldsymbol{\theta})\right]\right)\mathbf{s}^\dagger(\mathbf{y};\boldsymbol{\theta})\right\} \tag{A-9}$$

Here, Equation (A-8) follows from the properties of expectation [5] and Equation (A-9) from the fact that $\mathbf{s}(\mathbf{y};\boldsymbol{\theta})$ does not depend upon $\boldsymbol{\alpha}$. To simplify $E_{\boldsymbol{\alpha}|\mathbf{y}}\left[\mathbf{s}(\mathbf{y}|\boldsymbol{\alpha};\boldsymbol{\theta})\right]$ from Equation (A-9), we will exploit properties of the conditional and unconditional scores given by Equations (A-2) and (A-3), respectively. Recall from Bayes' theorem [5] that we have

$$p(\mathbf{y}|\boldsymbol{\alpha};\boldsymbol{\theta}) = \frac{p(\boldsymbol{\alpha}|\mathbf{y};\boldsymbol{\theta})p(\mathbf{y};\boldsymbol{\theta})}{p(\boldsymbol{\alpha})} \tag{A-10}$$

In Equation (A-10), we implicitly assume that $\boldsymbol{\alpha}$ does not depend upon the parameter vector $\boldsymbol{\theta}$. Using Equation (A-10) in Equation (A-2) leads to the following:

$$\mathbf{s}(\mathbf{y}|\boldsymbol{\alpha};\boldsymbol{\theta}) = \nabla_{\boldsymbol{\theta}}\left[\ln p(\boldsymbol{\alpha}|\mathbf{y};\boldsymbol{\theta}) + \ln p(\mathbf{y};\boldsymbol{\theta}) - \ln p(\boldsymbol{\alpha})\right]$$

$$= \mathbf{s}(\mathbf{y};\boldsymbol{\theta}) + \nabla_{\boldsymbol{\theta}} \ln p(\boldsymbol{\alpha}|\mathbf{y};\boldsymbol{\theta}) \tag{A-11}$$

To arrive at Equation (A-11), we used the definition given in Equation (A-3) in addition to the assumption that $\boldsymbol{\alpha}$ does not depend on $\boldsymbol{\theta}$. Taking the expectation of both sides of Equation (A-11) with respect to $\boldsymbol{\alpha}|\mathbf{y}$ leads to the following chain of equalities:

$$\begin{aligned}
E_{\boldsymbol{\alpha}|\mathbf{y}}\left[\mathbf{s}(\mathbf{y}|\boldsymbol{\alpha};\boldsymbol{\theta})\right] &= E_{\boldsymbol{\alpha}|\mathbf{y}}\left[\mathbf{s}(\mathbf{y};\boldsymbol{\theta})\right] + E_{\boldsymbol{\alpha}|\mathbf{y}}\left[\nabla_{\boldsymbol{\theta}} \ln p(\boldsymbol{\alpha}|\mathbf{y};\boldsymbol{\theta})\right] \\
&= \mathbf{s}(\mathbf{y};\boldsymbol{\theta}) + \int_{\mathcal{R}_{\boldsymbol{\alpha}|\mathbf{y}}} \left[\nabla_{\boldsymbol{\theta}} \ln p(\boldsymbol{\alpha}|\mathbf{y};\boldsymbol{\theta})\right] p(\boldsymbol{\alpha}|\mathbf{y};\boldsymbol{\theta})\, d\boldsymbol{\alpha} \qquad \text{(A-12)} \\
&= \mathbf{s}(\mathbf{y};\boldsymbol{\theta}) + \int_{\mathcal{R}_{\boldsymbol{\alpha}|\mathbf{y}}} \nabla_{\boldsymbol{\theta}}\, p(\boldsymbol{\alpha}|\mathbf{y};\boldsymbol{\theta})\, d\boldsymbol{\alpha} \qquad \text{(A-13)} \\
&= \mathbf{s}(\mathbf{y};\boldsymbol{\theta}) + \nabla_{\boldsymbol{\theta}} \left[\int_{\mathcal{R}_{\boldsymbol{\alpha}|\mathbf{y}}} p(\boldsymbol{\alpha}|\mathbf{y};\boldsymbol{\theta})\, d\boldsymbol{\alpha}\right] \qquad \text{(A-14)} \\
&= \mathbf{s}(\mathbf{y};\boldsymbol{\theta}) + \nabla_{\boldsymbol{\theta}}\left[1\right] = \mathbf{s}(\mathbf{y};\boldsymbol{\theta}) \qquad \text{(A-15)}
\end{aligned}$$

Here, Equation (A-12) follows from the fact that $\mathbf{s}(\mathbf{y};\boldsymbol{\theta})$ does not depend upon $\boldsymbol{\alpha}$ and the definition of expectation, while Equation (A-13) follows from differentiating the logarithm. Equation (A-14) follows from interchanging the orders of integration and differentiation (which is allowable here as $\boldsymbol{\alpha}$ and $\boldsymbol{\theta}$ are independent of each other [5]), whereas Equation (A-15) follows from the fact that any pdf integrates to unity over its region of support [5].

Substituting Equation (A-15) into Equation (A-9) leads to the following simplified expression for the quantity $E_{\mathbf{y},\boldsymbol{\alpha}}\left[\mathbf{s}(\mathbf{y}|\boldsymbol{\alpha};\boldsymbol{\theta})\mathbf{s}^{\dagger}(\mathbf{y};\boldsymbol{\theta})\right]$:

$$E_{\mathbf{y},\boldsymbol{\alpha}}\left[\mathbf{s}(\mathbf{y}|\boldsymbol{\alpha};\boldsymbol{\theta})\mathbf{s}^{\dagger}(\mathbf{y};\boldsymbol{\theta})\right] = \mathbf{H}(\boldsymbol{\theta}) \qquad \text{(A-16)}$$

Similarly, we can show that $E_{\mathbf{y},\boldsymbol{\alpha}}\left[\mathbf{s}(\mathbf{y};\boldsymbol{\theta})\mathbf{s}^{\dagger}(\mathbf{y}|\boldsymbol{\alpha};\boldsymbol{\theta})\right] = \mathbf{H}(\boldsymbol{\theta})$ as well. Using Equation (A-16) and this last result in Equation (A-7) leads to the following simplified expression for the autocorrelation matrix $\mathbf{K}(\boldsymbol{\theta})$:

$$\mathbf{K}(\boldsymbol{\theta}) = \mathbf{G}(\boldsymbol{\theta}) - \mathbf{H}(\boldsymbol{\theta}) \qquad \text{(A-17)}$$

As $\mathbf{K}(\boldsymbol{\theta}) \geq \mathbf{0}$, from Equation (A-17), it is clear that Equation (A-1) follows. This completes the proof.